Metabolic Mechanism of Delamanid, a New Anti-Tuberculosis Drug, in Human Plasma

２０１５年

下川　義彦

Table of Contents

List of Abbreviations

$AUC_{0\text{-}24h}$	:	area under the plasma concentration–time curve from 0 to 24 h
$AUC_{0\text{-}t}$	:	area under the plasma concentration–time curve calculated to the last observable concentration at time t
$AUC_{0\text{-}\infty}$	:	area under the concentration–time curve from time zero to infinity
CYP	:	cytochrome P450
C_{max}	:	maximum plasma concentration
DDI	:	drug–drug interaction
DMSO	:	dimethyl sulfoxide
DSA	:	dog serum albumin
GAPDH	:	glyceraldehyde-3-phosphate dehydrogenase
HIV	:	human immunodeficiency virus
HPLC	:	high-performance liquid chromatography
HPRT1	:	hypoxanthine phosphoribosyltransferase 1
HSA	:	human serum albumin
ICR	:	Institute of Cancer Research
LC-MS/MS	:	liquid chromatography-tandem mass spectrometry
LSC	:	liquid scintillation counter
MBI	:	mechanism-based inactivation
MDR-TB	:	multidrug-resistant tuberculosis
$MRT_{0\text{-}\infty}$	:	mean residence time from time zero to infinity
MS	:	mass spectrometry
NAD	:	nicotinamide adenine dinucleotide phosphate
NADH	:	reduced nicotinamide adenine dinucleotide

NADPH	:	reduced nicotinamide adenine dinucleotide phosphate
RSA	:	rat serum albumin
SD	:	Sprague–Dawley
TB	:	tuberculosis
UV	:	ultraviolet
WHO	:	World Health Organization
$t_{1/2,z}$	:	terminal-phase elimination half-life
t_{max}	:	time to maximum (peak) plasma concentration

Chapter 1

General Introduction

Tuberculosis (TB) is a contagious bacterial infection caused by *Mycobacterium tuberculosis*, a pathogen that most commonly affects the lungs. TB is global health problem. In 2013, an estimated 9.0 million people developed TB and 1.5 million died from the disease [World Health Organization (WHO), (http://apps.who.int/iris/bitstream/10665/137094/1/ 9789241564809_eng.pdf)]. Multidrug-resistant TB (MDR-TB) is defined as infection with a strain of *Mycobacterium tuberculosis* that is resistant to at least the first-line drugs isoniazid and rifampicin (Chang et al., 2013). The increasing occurrence of MDR-TB and human immunodeficiency virus (HIV) co-infection is an important driver of the current TB epidemic. The mortality of patients co-infected with HIV and MDR-TB can exceed 60% (Gandhi et al., 2012). Current treatment regimens for MDR-TB are more toxic, last longer, and are less effective than treatment regimens for drug-sensitive TB (Falzon et al., 2011). Thus, there is an urgent need to develop shorter-acting and less toxic regimens to reduce the side effects and mortality associated with MDR-TB chemotherapy. According to a WHO guideline published in 2011 (http://whqlibdoc.who.int/publications/2011/ 9789241501583_eng.pdf), a novel drug for drug-resistant TB should be used for long-term administration as an add-on therapy to at least 3 or more other anti-TB drugs to prevent the development of resistance.

Delamanid, (*R*)-2-methyl-6-nitro-2-[(4-{4-[4-(trifluoromethoxy)phenoxy]piperidin-1-yl}phenoxy)methyl]-2,3-dihydroimidazo[2,1-*b*]oxazole, (Fig. 1-1) was synthesized by Otsuka Pharmaceutical Co., Ltd. as a new anti-TB agent (Sasaki et al., 2006). Delamanid inhibits mycolic acid synthesis by *Mycobacterium tuberculosis* and has shown potent pre-clinical *in vitro* and *in vivo* activities against both drug-susceptible and drug-resistant strains (Matsumoto et al., 2006).

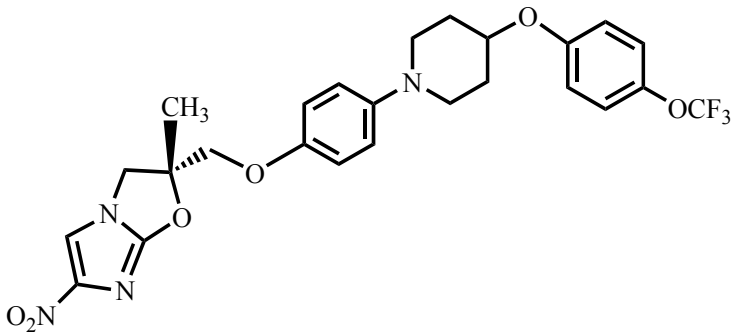

Fig. 1-1 Chemical structure of delamanid.

Further, delamanid has demonstrated anti-TB activity and a favorable safety profile in patients with drug-sensitive TB (Diacon et al., 2011) and MDR-TB, and is currently being tested as a specific treatment for MDR-TB infections (Gler et al., 2012; Skripconoka et al., 2013). In 2014, delamanid was approved as adjunct therapy for adults with pulmonary MDR-TB by the European Medicines Agency, the Ministry of Health, Labor and Welfare of Japan, and the Korean Food and Drug Administration.

With the background of delamanid in pre-clinical and clinical pharmacology, we investigated the *in vivo* pharmacokinetics and metabolism of delamanid in humans and animals (mouse, rat, and dog) in Chapter 2. The *in vitro* metabolism of delamanid using human and animal liver microsomes has already been evaluated (Matsumoto et al., 2006). When delamanid was incubated with liver microsomes in the presence of reduced nicotinamide adenine dinucleotide phosphate (NADPH), metabolites were nearly undetectable in the incubation mixture, suggesting that delamanid was not metabolized by cytochrome P450 (CYP) enzymes. However, eight metabolites, including the abundant metabolite (*R*)-2-amino-4,5-dihydrooxazole derivative (M1), in human and animal plasma were detected and identified in the investigation for the *in vivo* pharmacokinetics and metabolism of delamanid, as described in Chapter 2. The maximum plasma concentration (C_{max}) of M1 was nearly half that of delamanid (0.32 μM vs. 0.78 μM) following twice daily

administration of 100 mg delamanid for 56 days (Gler et al., 2012; Chapter 2), suggesting that M1 is the major metabolite. On the basis of the chemical structure of M1, it is proposed that delamanid is cleaved directly at its 6-nitro-2,3-dihydro-imidazo[2,1-*b*]oxazole moiety by some extrahepatic mechanism (Matsumoto et al., 2006). It is important to identify the enzymes responsible for the metabolism of delamanid in humans. We examined the *in vitro* metabolism of delamanid using plasma and purified protein preparations to clarify the metabolic mechanism to form M1 in Chapter 3.

Individuals who are coinfected with HIV and *Mycobacterium tuberculosis* may require treatment with a number of medications that might interact significantly with the CYP enzyme system as inhibitors or inducers. It is therefore important to understand how drugs in development for the treatment of TB will affect CYP enzyme metabolism. The ability of delamanid to inhibit and induce CYP enzymes was investigated *in vitro* using human liver microsomes and human hepatocytes in Chapter 4. Furthermore, information on the CYP inhibitory potential for anti-TB drugs both *in vivo* and *in vitro* is limited. It is therefore critical to understand the ability of anti-TB drugs to inhibit CYP enzymes. In Chapter 5, twenty five anti-TB drugs were selected by reference to the WHO guideline published in 2011, and the direct inhibitory effects of these anti-TB drugs on CYP enzymes were evaluated using human liver microsomes *in vitro*.

Chapter 2

In Vivo Pharmacokinetics and Metabolism of Delamanid in Animals and Humans

2.1. Objectives

It is important to understand the pharmacokinetic and metabolic profiles for new drugs in animals and humans so that the impact on efficacy and safety can be interpreted or predicted. In this study, we investigated the metabolites, the metabolic pathways, interspecies pharmacokinetics, and CYP enzymes that catabolize delamanid and characterized the pharmacokinetics and metabolism of delamanid in animals and humans.

2.2. Materials and Methods

2.2.1. Materials

Delamanid and its metabolites, M1 to M8, were supplied by Otsuka Pharmaceutical Co., Ltd. Microsomes prepared from baculovirus-infected insect cells expressing recombinant human CYP1A1, CYP1A2, CYP2A6, CYP2B6, CYP2C8, CYP2C9, CYP2C19, CYP2D6, CYP2E1, CYP3A4, and CYP3A5 were obtained from Becton Dickinson and Company. Human liver microsomes were obtained from XenoTech LLC. Furafylline, ticlopidine, sulfaphenazole, quinidine, ketoconazole, Tris–HCl buffer (pH 7.4), reduced nicotinamide adenine dinucleotide (NADH), and NADPH were purchased from Sigma-Aldrich Co. Benzylnirvanol was purchased from Toronto Research Chemicals, Inc. Human serum was prepared from blood samples of 3 healthy male volunteers after approval by the Institutional Ethics Committee. Mouse (Institute of Cancer Research; ICR), rat (Sprague–Dawley; SD), and dog (beagle) sera were supplied from Kitayama Labes Co. Phosphate buffer (pH 7.4) was purchased from Nacalai Tesque, Inc. Other reagents and solvents were either special or high-performance liquid chromatography (HPLC) grade.

2.2.2. Animals and Humans

Male ICR mice at 4 or 5 weeks of age were supplied from Japan SLC, Inc. or Charles River Laboratories Japan, Inc. Male SD rats at 5 weeks of age were supplied from Charles River Laboratories Japan, Inc. Male and female beagle dogs at 6 months old were supplied from Covance Research Products, Inc. Environmental conditions were set to maintain an air-exchange rate of 13–17 times/h and maintained at 18°C to 26°C with 30% to 80% relative humidity in the housing room that was lighted for 12 h (7:00–19:00) daily. Animals were individually housed and allowed free access to tap water via an automatic water supply system. Male mice and rats were provided with pelleted food (CRF-1, sterilized by radiation; Oriental Yeast Co., Ltd.) *ad libitum*. Male and female dogs were supplied with 300 g/day of pellet diet (DS-A; Oriental Yeast Co., Ltd. or CD-5M; Clea Japan, Inc.).

The animal experimental protocols and procedures were reviewed in accordance with Guidelines for Animal Care and Use in Otsuka Pharmaceutical Co., Ltd. and approved by the in-house Animal Ethics Committee. The human trial protocol, available with the full text of another report (Gler et al., 2012), was approved by independent ethics committees and institutional review boards for all sites. All male healthy volunteers and male and female patients provided written informed consent in their native language before enrollment. The trial was performed in accordance with the Good Clinical Practice guidelines of the International Conference on Harmonization (ICH-GCP), adhered to the ethical principles of the Declaration of Helsinki, and was monitored by an independent data and safety monitoring committee.

2.2.3. Investigation of Metabolites

After repeated dosing at 100 mg/kg/day for 14 days to 6 male mice and 3 male rats, blood was withdrawn into heparinized syringes at 8 h and 24 h. Blood from male and female dogs (n = 3, each sex) was withdrawn into heparinized syringes at 24 h after the final oral dosing at 100 mg/kg/day for 13 weeks. After centrifugation at approximately 1700 × *g* for 10 min at 4°C, the supernatants were stored at −15°C or below until use. Plasma samples for each sex and at each sampling point were equally mixed. After the plasma sample was mixed with an equal volume of acetonitrile, the mixture was centrifuged at 12000 × *g* for 5 min at 4°C. A 5-μL aliquot of the supernatant was analyzed by liquid chromatography-tandem mass spectrometry (LC-MS/MS). In addition, another 0.6-mL aliquot of the plasma sample was extracted with 5 mL of ethyl acetate by shaking for 10 min. After centrifugation as above, the organic layer was evaporated to dryness at 40°C. The residue was dissolved in 0.1 mL of acetonitrile/water (100:1, *v/v*) and sonicated, and then a 5-μL aliquot of the resulting solution was analyzed by LC-MS/MS and monitored by ultraviolet (UV) detection at 254 nm. Liquid chromatography used a TSKgel ODS-80Ts column (150 mm × 2.0 mm i.d., 5 μm, Tosoh Corp.) with a binary gradient solvent system consisting of A: water/acetic acid (100:1, *v/v*) and B: acetonitrile/ acetic acid (100:1, *v/v*); the chromatography was performed using a Nanospace SI-2 HPLC system (Shiseido Co., Ltd.). The column temperature was maintained at 40°C, and the flow rate was 0.2 mL/min. LC eluate was introduced directly into an API3000 triple-quadrupole mass spectrometer (AB SCIEX), equipped with an electrospray ionization interface operated in positive-ion mode with the following operation parameters: gas temperature, 475°C; gas flow rate, 7 L/min; gas pressure, 70 psi; ion-spray voltage, 4.5 kV; nebulizer gas, 12 units; curtain gas, 8 units; and collision gas, 8 units. Nitrogen was used in the ion source and the collision cell. A full scan from *m/z* 200 to 700, a precursor ion scan at *m/z* 352, and a product-ion scan from the protonated molecules ($[M+H]^+$) of analytes were

performed.

2.2.4. Exposure to Delamanid and its Metabolites

Animal blood samples in the single-dose pharmacokinetic study were collected as follows: 1, 2, 4, 6, 8, 12, 24, 32, 48, 72, 96, 144, 192, 288, and 480 h after the single dosing at 3 mg/kg in mice and rats (n = 3) and 2, 4, 6, 8, 12, 24, 32, 48, 72, 96, 144, 192, 240, 288, 384, 480, 576, and 768 h after the single dosing at 10 mg/kg in dogs (n = 4). In the repeated dose study, the animal blood was collected at 2, 4, 6, 8, and 24 h on day 1 (mice and rats, n = 3), at 13 weeks (mice, n = 3), and 26 weeks (rats, n = 3), and 2 and 6 h on day 1 (dogs, n = 4), and 1, 2, 6, 8, and 24 h at 39 weeks (dogs, n = 4) after oral dosing at 30 mg/kg/day. Blood samples in the single-dose pharmacokinetic study were collected at 0, 1, 2, 3, 4, 5, 6, 8, 12, 24, 48, 72, 96, 120, 144, and 168 h after the single dosing at 100 mg in human healthy volunteers (n = 6). Further, human bloods were withdrawn at 0, 2, 3, 4, 10, 12, 13, 14, and 24 h after oral dosing on days 1, 14, 28, and 56 after oral dosing at 100 mg bis in die (BID; twice a day) in patients (n = 144).

The blood samples were immediately placed in an ice bath and centrifuged at 1800 g for >10 min at 4°C to obtain plasma. The plasma samples were stored at −15°C or below until assay. The plasma concentrations of delamanid and its metabolites were simultaneously determined by LC-MS/MS and validated according to Food and Drug Administration guidance, including selectivity, accuracy, precision, recovery, calibration curve, post-preparative stability, freeze–thaw stability, short-term stability, and long-term stability. The sample analyses were performed under the optimal conditions of stability. The following typical method for the analysis of animal samples was used: to a 0.1-mL aliquot of plasma sample in an ice-water bath, 20 μL of internal standard solution (1 μg/mL, in-house

compound) and 0.1 mL of phosphate buffer (0.2 M, pH 7.0) were added. The mixture was extracted with 8 mL of *tert*-butyl methyl ether by shaking for 5 min. After centrifugation, the organic layer was evaporated to dryness under a stream of nitrogen at 40°C. The residue was dissolved in 0.15 mL of methanol/water/formic acid (50:50:1 *v/v/v*) and sonicated, and then a 5-μL aliquot of the resulting solution was analyzed by LC-MS/MS. Separation of the analytes was achieved with a SunFire C_{18} column (50 mm × 2.1 mm i.d., 3.5 μm; Waters Corp.) using a Waters 600S HPLC system (Waters Corp.). The mobile phases were 1 mM ammonium formate/formic acid (1000:2, *v/v*) (solvent A) and methanol (solvent B). The column temperature was maintained at room temperature, and the HPLC system was set to operate at a flow rate of 0.25 mL/min under linear-gradient conditions. The HPLC eluate was introduced directly into a triple-quadrupole mass spectrometer, TSQ-7000 (Thermo Fisher Scientific, Inc.), and the mass spectrometer was operated in the positive electrospray ionization selected reaction monitoring (SRM) mode. The SRM mode was used with the following transitions: delamanid, *m/z* 535.2→352; M1, *m/z* 466.2→352; M2, *m/z* 482.2→352; M3, *m/z* 480.2→352; M4, *m/z* 467.2→352; M5, *m/z* 484.2→352; M6 and M7, *m/z* 483.2→305; and M8, *m/z* 481.2→305. The other parameters were as follows: spray voltage, 4.5 kV; electron-multiplier voltage, 1.45 kV; nitrogen sheath gas pressure, 80 psi; nitrogen auxiliary gas pressure, 10 (arbitrary units); argon collision gas pressure, 2.0 mTorr; capillary temperature, 260°C. Data acquisition and processing were performed using Xcalibur software version 1.2 (Thermo Fisher Scientific Inc.). The calibration curve ranges of delamanid for mouse, rat, and dog plasma were 6–2000 ng/mL, 3–1000 ng/mL, and 3–1000 ng/mL, respectively, and those of the metabolites were 6–600 ng/mL, 3–300 ng/mL, and 3–1000 ng/mL, respectively. In humans, the concentrations of delamanid and its metabolites were determined using previously published LC-MS/MS methods after extraction by protein precipitation (Gler et al., 2012).

The pharmacokinetic parameters, C_{max}, time to maximum (peak) plasma concentration (t_{max}), area under the plasma concentration–time curve from 0 to 24 h (AUC_{0-24h}), area under the plasma concentration–time curve calculated to the last observable concentration at time t (AUC_{0-t}), area under the concentration–time curve from time zero to infinity ($AUC_{0-\infty}$), mean residence time from time zero to infinity ($MRT_{0-\infty}$), and terminal-phase elimination half-life ($t_{1/2,z}$) were calculated with the aid of WinNonlin software (version 5.0.1 or 5.2, noncompartmental model; Pharsight Corp.).

2.2.5. Identification of Human Cytochrome P450 Isoforms

For recombinant studies, the following recombinant microsomes were used in duplicate: CYP1A1, CYP1A2, CYP2A6, CYP2B6, CYP2C8, CYP2C9, CYP2C19, CYP2D6, CYP2E1, CYP3A4, and CYP3A5. Each incubation contained recombinant microsomes (0.7 mg/mL, 50 nM of CYP protein), phosphate buffer (100 mM, pH 7.4), metabolites (10 μM M1 or M2), NADPH (2.5 mM), and NADH (2.5 mM) in a total volume of 0.5 mL. Incubation mixtures were pre-incubated at 37°C for 5 min, and reactions were started by adding a mixture of NADPH and NADH. After 0, 10, and 30 min of incubation at 37°C, the reactions were terminated with 1 mL of acetonitrile, containing the internal standard (IS; in-house compound). After centrifugation, the supernatant was analyzed by LC-MS/MS.

For chemical inhibition studies, the following inhibitors were used in duplicate: furafylline (CYP1A2), ticlopidine (CYP2B6), sulfaphenazole (CYP2C9), benzylnirvanol (CYP2C19), quinidine (CYP2D6), and ketoconazole (CYP3A4). Each incubation contained human liver microsomes (1.0 mg/mL), inhibitors (0, 1, and 10 μM), phosphate buffer (100 mM, pH 7.4), metabolites (10 μM M1 or M2), NADPH (2.5 mM), and NADH (2.5 mM) in a total volume of 0.5 mL. Incubation mixtures were preincubated at 37°C for 5 min, and

reactions were started by adding a mixture of NADPH and NADH. For furafylline and ticlopidine, the prereaction was performed without delamanid derivative for 15 min. Reactions were performed at 37°C for a set time period within the time linearity limit (M2 from M1 for 40 min and M3 from M2 for 180 min). After the addition of 1 mL of acetonitrile containing IS, the solution was centrifuged, and the supernatant was analyzed by LC-MS/MS, referring to the animal methods.

2.2.6. Binding of Metabolites to Serum

The *in vitro* binding of M1, M4, and M5 at the concentrations of 500 and 5000 ng/mL to animal and human sera was determined by equilibrium dialysis using a Spectra/Por2 molecular porous dialysis membrane (Spectrum Laboratories, Inc.). Because M1, M4 and M5, unlike delamanid, are stable in the serum at 37°C, equilibrium dialysis was conducted under the condition for 8 h at 37°C. After dialysis for protein binding, an aliquot of the dialyzed protein and dialysate in the 2 devices was sampled to determine the concentrations in the bound and unbound fractions. Cooled *tert*-butyl ether (mouse and rat) or diethyl ether (dog and human) containing IS was added to the sample and shaken for >5 min. The organic layer was evaporated, and the residue was dissolved in water/methanol/formic acid (50:50:1, *v/v/v*). The supernatant was analyzed using the modified LC-MS/MS method as described above.

2.3. Results

2.3.1. Investigation of Metabolites in Plasma

Initially we performed full-scan LC-MS analysis using the plasma extracts from mice, rats, and dogs following repeated oral doses of delamanid, but no peaks were detected. Delamanid formed the $[M + H]^+$ at *m/z* 535 in positive-ion scan mode, and the fragment ions of delamanid were mainly observed at *m/z* 352 in the product-ion scan at *m/z* 535. Therefore, a precursor-ion scan at *m/z* 352 was performed, and 8 metabolites, M1 to M8, were detected in male dog plasma (Fig. 2-1A), as well as female one. Sex difference was not observed. The intensities of these peaks monitored at UV 254 nm were much lower than the intensity of delamanid, and no other remarkable peak was observed in the dogs (Fig. 2-1B). In addition, the mouse and rat plasma also showed no remarkable metabolites other than M1 to M8 (data not shown). The chemical structures of these metabolites were determined by matching retention times, parent *m/z* ions, and MS/MS fragmentation patterns with those of the authentic compounds (Table 2-1).

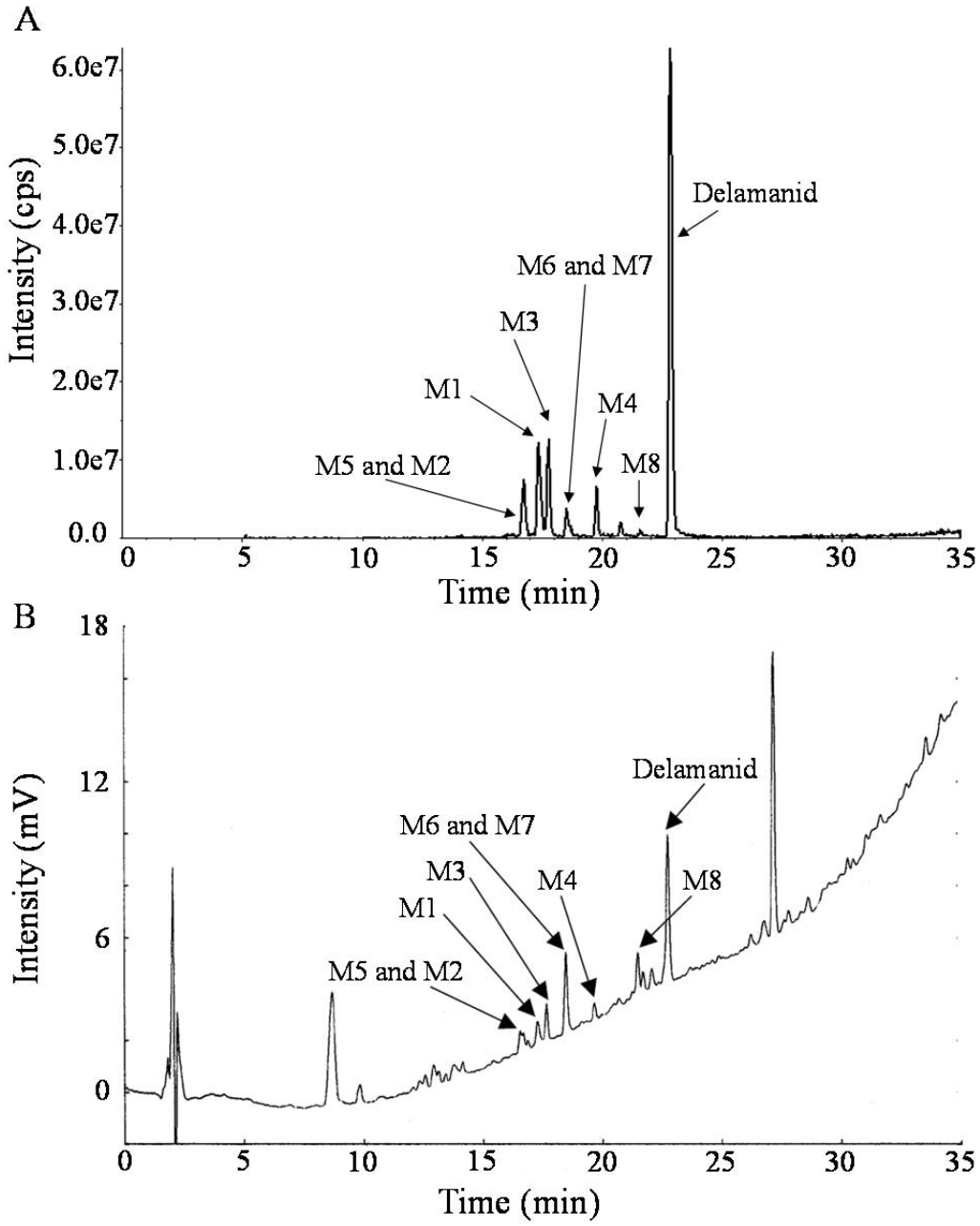

Fig. 2-1 Chromatograms of the precursor-ion scan at *m/z* 352 (A) and LC-UV at 254 nm (B) obtained from extracted dog plasma. Plasma was collected at 24 h after daily oral dosing of delamanid at 100 mg/kg/day for 13 weeks.

Table 2-1 Identified metabolites of delamanid.

Metabolite	Retention Time (min)	Chemical formula	Molecular weight	Structure and MS/MS product ions
Delamanid	22.8	$C_{25}H_{25}F_3N_4O_6$	534.48	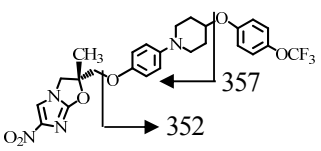
M1	17.3	$C_{23}H_{26}F_3N_3O_4$	465.47	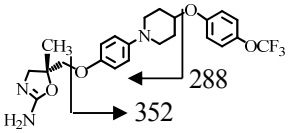
M2	16.7	$C_{23}H_{26}F_3N_3O_5$	481.46	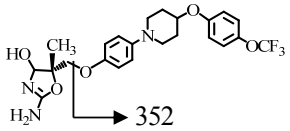
M3	17.8	$C_{23}H_{24}F_3N_3O_5$	479.45	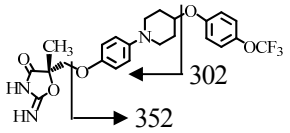
M4	19.8	$C_{23}H_{25}F_3N_2O_5$	466.45	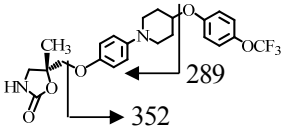
M5	16.7	$C_{23}H_{28}F_3N_3O_5$	483.48	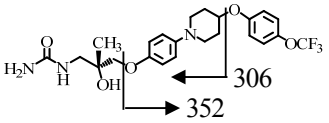
M6 and M7	18.6	$C_{23}H_{25}F_3N_2O_6$	482.45	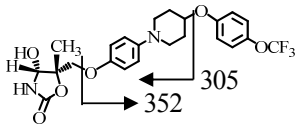 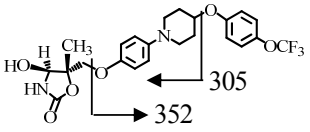
M8	21.6	$C_{23}H_{23}F_3N_2O_6$	480.43	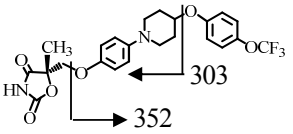

2.3.2. Single-dose Pharmacokinetics of Delamanid and Metabolites

Fig. 2-2 and Table 2-2 present information characterizing the pharmacokinetic behavior of an oral dose of delamanid in mice, rats, and dogs. After the administration of a single 3 mg/kg delamanid to mice, the maximum plasma concentration of delamanid (478.7 ng/mL) occurred at 2 h, followed by a decline in the plasma level with elimination $t_{1/2,z}$ of 7.2 h. In the rats, delamanid (3 mg/kg) absorption had a t_{max} of 4 h and a C_{max} of 600.5 ng/mL. The $t_{1/2,z}$ (5.1 h) was similar to that obtained in the mice. In the dogs treated with oral delamanid (10 mg/kg), the t_{max} and C_{max} were 8 h and 357.8 ng/mL, respectively. The $t_{1/2,z}$ in dogs was 18.4 h, which was longer than that in the rodents. In all animal species, the plasma concentrations of the delamanid metabolites were much less than the concentration of the parent compound. The metabolites appeared slowly in plasma, and had very long MRT and elimination half-lives in the dogs (Figs. 2-2C-1 and 2-2C-2), particularly M2, M3, and M8 (t_{max}: 156–456 h, $MRT_{0-\infty}$: 413.8–1488.0 h, $t1_{/2,z}$: 229.2–884.2 h).

Fig. 2-3 and Table 2-2 show the plasma profiles and pharmacokinetic parameters in humans. The C_{max} of delamanid reached 201 ng/mL at 4 h and thereafter decreased with the $t_{1/2,z}$ of 25.6 h.

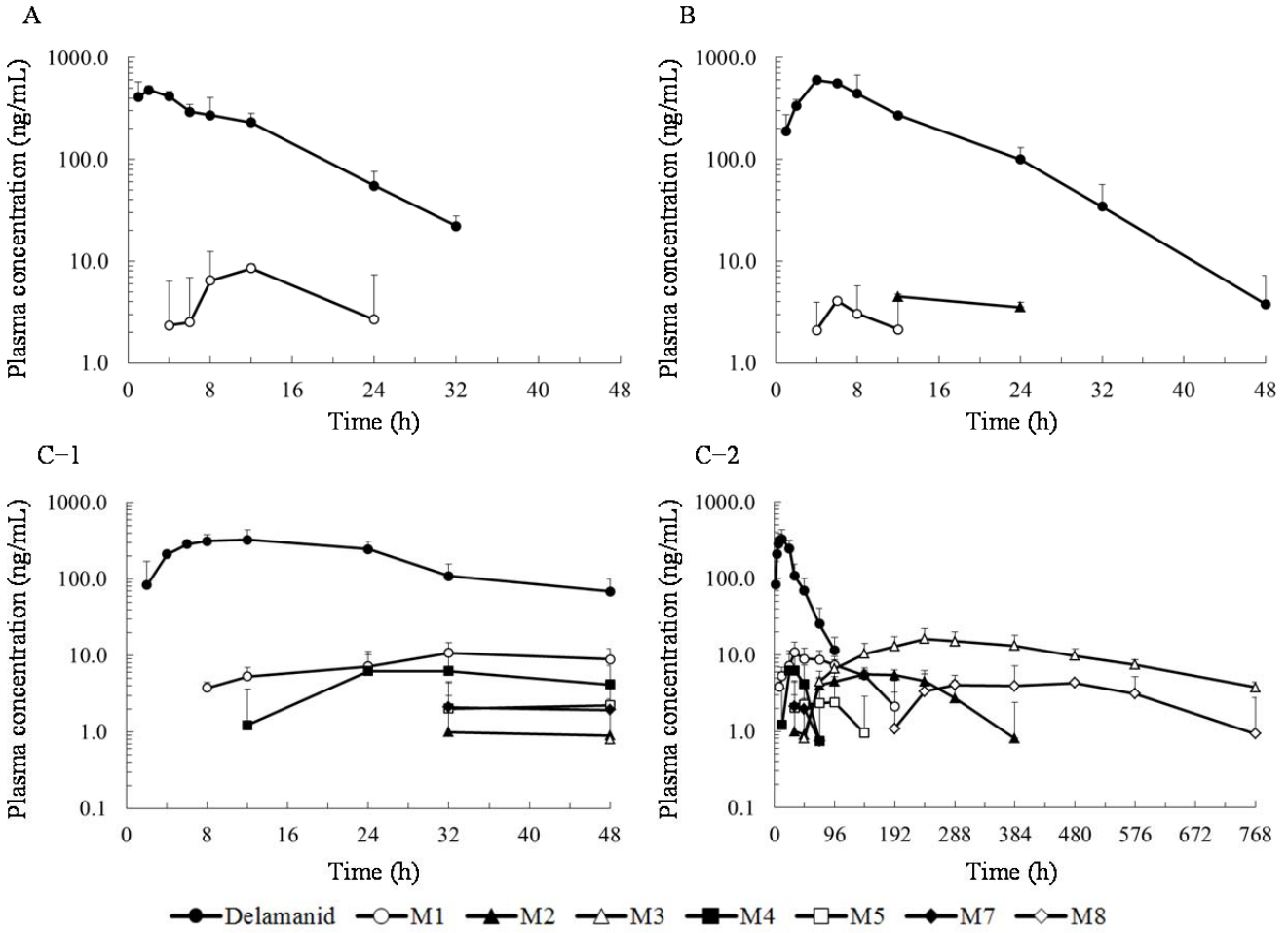

Fig. 2-2 Plasma concentration–time profiles of delamanid and its metabolites in mice (A), rats (B), and dogs (C).
Delamanid was administered orally at single doses of 3 mg/kg (mice and rats, *n* = 3) and 10 mg/kg (dogs, *n* = 4). The horizontal axis represents time after administration from 0 to 48 h (A, B, C-1) and to 768 h (C-2). Each data point represents the mean + standard deviation.

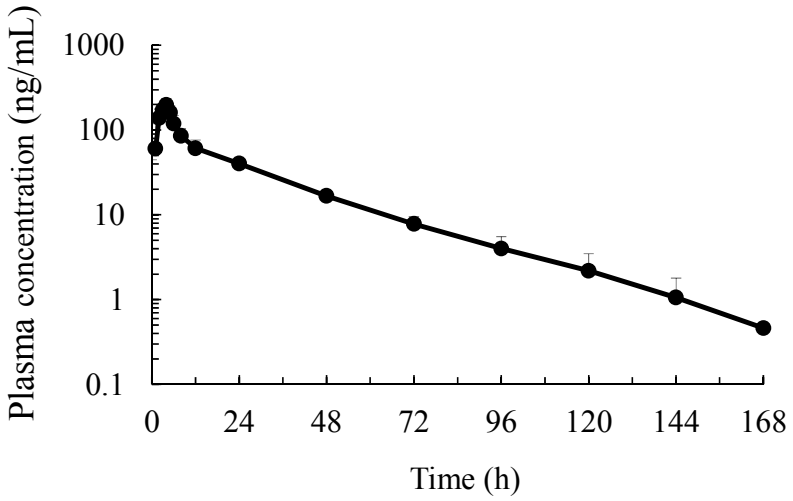

Fig. 2-3 Plasma concentration–time profiles of delamanid in human. Delamanid was administered orally at a single dose of 100 mg (*n* = 6). Each data point represents the mean + standard deviation.

Table 2-2 Pharmacokinetic parameters of delamanid and its metabolites after single oral administration in the mouse, rat, dog, and human.

Species (Dose)	Metabolite	C_{max} (ng/mL)	t_{max} (h)	AUC_{0-t} (ng·h/mL)	$AUC_{0-\infty}$ (ng·h/mL)	$MRT_{0-\infty}$ (h)	$t_{1/2,z}$ (h)
Mouse	Delamanid	478.7	2	5536.0	6150.8	10.8	7.2
(3 mg/kg)	M1	8.5	12	113.0	NC	NC	NC
Rat	Delamanid	600.5	4	7941.8	7969.8	11.2	5.1
(3 mg/kg)	M1	4.1	6	25.6	44.6	13.3	6.4
	M7	4.5	12	57.0	NC	NC	NC
Dog	Delamanid	357.8	8	10628.0	10927.5	27.6	18.4
(10 mg/kg)	M1	10.9	36	1158.9	1850.1	174.9	108.0
	M2	6.0	156	1155.6	2433.9	413.8	229.2
	M3	16.3	240	6966.1	8272.3	491.4	233.7
	M4	6.6	27	214.3	495.6	63.4	30.8
	M5	2.6	84	205.6	1286.0	229.5	134.4
	M7	2.1	32	64.2	501.6	122.4	65.8
	M8	5.2	456	1582.8	6940.3	1488.0	884.2
Human (100 mg)	Delamanid	201	4.0	NC	3191	NC	25.6

NC: not calculated Values are the mean of *n* = 3 (mouse and rat), *n* = 4 (dog), and *n* = 6 (human). Data for quantified metabolites are summarized.

2.3.3. Multiple-dose Pharmacokinetics of Delamanid and Metabolites

Table 2-3 lists the mouse, rat, dog, and human C_{max} and AUC values. The C_{max} of delamanid in male mouse plasma reached 2920.9 ng/mL at 6 h after repeated administration of 30 mg/kg/day. The C_{max} in the male rat plasma reached 1799.2 ng/mL at 4 h. The extent of delamanid absorption (C_{max} and AUC) did not alter significantly on multiple administrations in the mice and rats. The C_{max} of delamanid in male dog plasma reached 1400.7 ng/mL at 3 h after repeated administration at 30 mg/kg/day, and decreased with time. There was no remarkable difference between the ratios of delamanid between males and females in the rodents and dogs (data not shown). The C_{max} of delamanid in the human plasma reached 135 and 414 ng/mL at 4 h after single and repeated administration at 100 mg BID, respectively. Approximately 3.7- and 3.1-fold delamanid accumulation was observed after repeated administration in dogs and humans, respectively (Table 2-3, Fig. 2-4). There was no difference among the C_{max} and AUC values for delamanid on days 14 to 56 in humans; therefore, a steady-state delamanid concentration was reached at ≤14 days (Fig.2-4).

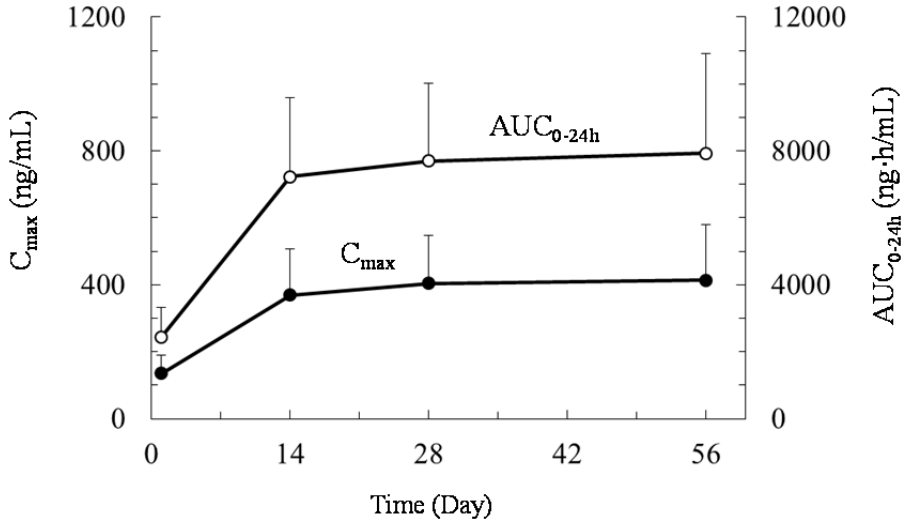

Fig. 2-4 Changes in C_{max} and AUC_{0-24h} of delamanid in humans during multiple administrations for 56 days. Delamanid was administered orally at 100 mg BID. Each data point represents the mean + standard deviation (n = 144). AUC_{0-24h} was calculated from the first dosing of BID on each day to 24 h.

Table 2-3 Species differences in the systemic exposure in the mouse, rat, dog, and human after initial or multiple oral administrations.

Species	Mouse				Rat				Dog				Human		
Dose (mg/kg/day)	30				30				30				100 mg BID		
Duration	Initial		13 Weeks		Initial		26 Weeks		Initial		39 Weeks		Initial		56 Days
No of subject	3		3		3		3		4		4		144		144
							C_{max} (ng/mL) [a]								
Delamanid	2314.1	(95)	2920.9	(90)	2695.3	(97)	1799.2	(82)	383.1 [b]	(95)	1400.7	(36)	135	414[c]	(42)
M1	66.6	(3)	135.6	(5)	26.2	(1)	40.7	(2)	5.3 [b]	(2)	523.6	(15)	NM	151	(17)
M2	2.4	(0)	25.7	(1)	ND	(0)	4.1	(0)	ND [b]	(0)	379.9	(11)	NM	57	(7)
M3	ND	(0)	2.0	(0)	ND	(0)	ND	(0)	ND [b]	(0)	536.6	(15)	NM	107	(12)
M4	2.8	(0)	10.3	(0)	2.8	(0)	13.0	(1)	3.1 [b]	(1)	134.3	(4)	NM	61	(7)
M5	10.6	(0)	46.8	(2)	6.1	(0)	33.6	(2)	8.9 [b]	(2)	126.8	(4)	NM	59	(7)
M6	ND	(0)	2.5	(0)	ND	(0)	18.7	(1)	ND [b]	(0)	54.0	(2)	NM	6	(1)
M7	23.8	(1)	74.4	(3)	39.8	(2)	215.3	(11)	ND [b]	(0)	53.2	(2)	NM	33	(4)
M8	ND	(0)	4.6	(0)	ND	(0)	32.5	(2)	ND [b]	(0)	423.5	(12)	NM	35	(4)
							$AUC_{0\text{-}24h}$ (ng·h/mL) [a]								
Delamanid	35840.3	(95)	36509.4	(85)	36639.7	(98)	34237.9	(82)	NC [d]		21769.2	(29)	2441	7925[c]	(40)
M1	1148.2	(3)	2512.8	(7)	409.2	(1)	792.7	(2)	NC [d]		11028.6	(17)	NM	3125	(18)
M2	19.2	(0)	496.4	(1)	NC	(0)	76.8	(0)	NC [d]		8050.1	(12)	NM	1206	(7)
M3	NC	(0)	4.0	(0)	NC	(0)	NC	(0)	NC [d]		11379.6	(17)	NM	2285	(13)
M4	29.4	(0)	111.5	(0)	25.2	(0)	256.7	(1)	NC [d]		2725.7	(4)	NM	1251	(7)
M5	109.1	(0)	957.1	(2)	48.8	(0)	645.2	(2)	NC [d]		2703.4	(4)	NM	1256	(7)
M6	NC	(0)	30.8	(0)	NC	(0)	329.2	(1)	NC [d]		1106.0	(2)	NM	132	(1)
M7	403.0	(1)	1443.7	(4)	380.1	(1)	3954.0	(10)	NC [d]		1151.0	(2)	NM	699	(4)
M8	NC	(0)	54.4	(0)	NC	(0)	682.6	(2)	NC [d]		8721.7	(13)	NM	720	(4)

[a] The molar ratio of each analyte to the total exposure (%) is shown in parentheses. [b] These values were calculated using higher concentration between two sampling points (2 or 6 h) [c] Data were reported by Gler et al. (2012). [d] AUC was not calculated because of an insufficient number of sampling points (2 or 6 h). ND, not detected; NM, not measured; NC, not calculated

Delamanid was metabolized into M1 to M8 in animals and humans. The metabolites accumulated in rodents and especially in dogs during repeated daily administration. The AUC level of each metabolite was ≤10% of the total exposure in the rodents even after multiple doses. Following oral administration of multiple doses of delamanid to the dogs and humans, delamanid metabolites M1 and M3 appeared predominantly in the plasma and accounted for about 17% of the total exposure in dogs and about 13%–18% in humans.

2.3.4. Identification of Human Cytochrome P450 Isoforms

The major circulating metabolites of delamanid in humans were M1 and M3. The metabolite M1 is considered to be produced from delamanid by extrahepatic metabolism. We further examined the types of CYP enzymes involved in the formation of M3 from M1 via M2 in humans using recombinant CYP enzymes and human liver microsomes with CYP inhibitors.

Among the 11 recombinant human CYP enzymes studied (CYP1A1, CYP1A2, CYP2A6, CYP2B6, CYP2C8, CYP2C9, CYP2C19, CYP2D6, CYP2E1, CYP3A4, and CYP3A5), CYP1A1, CYP3A4, CYP2D6, and CYP2E1 time-dependently catalyzed the hydroxylation of M1 to M2 (Fig. 2-5A). No production of M2 was detected in the other CYP expression microsomes. Furthermore, CYP1A1 and CYP3A4 showed time-dependent metabolism of M2 to M3, and in the other CYPs, no production of M3 was detected (Fig. 2-5B). The metabolic activity of hydroxylation and dehydrogenation in recombinant human CYP1A1 was the highest among the 11 recombinant human CYP enzymes examined.

In the assay containing specific inhibitors for CYP (furafylline, ticlopidine, sulfaphenazole, benzylnirvanol, quinidine, and ketoconazole), only ketoconazole inhibited the metabolism of M1 to M2 and M2 to M3 in a dose-dependent manner, whereas other

inhibitors were ineffective (Fig. 2-6). These results indicated that CYP3A4 was mainly responsible for M2 and M3 formations in humans.

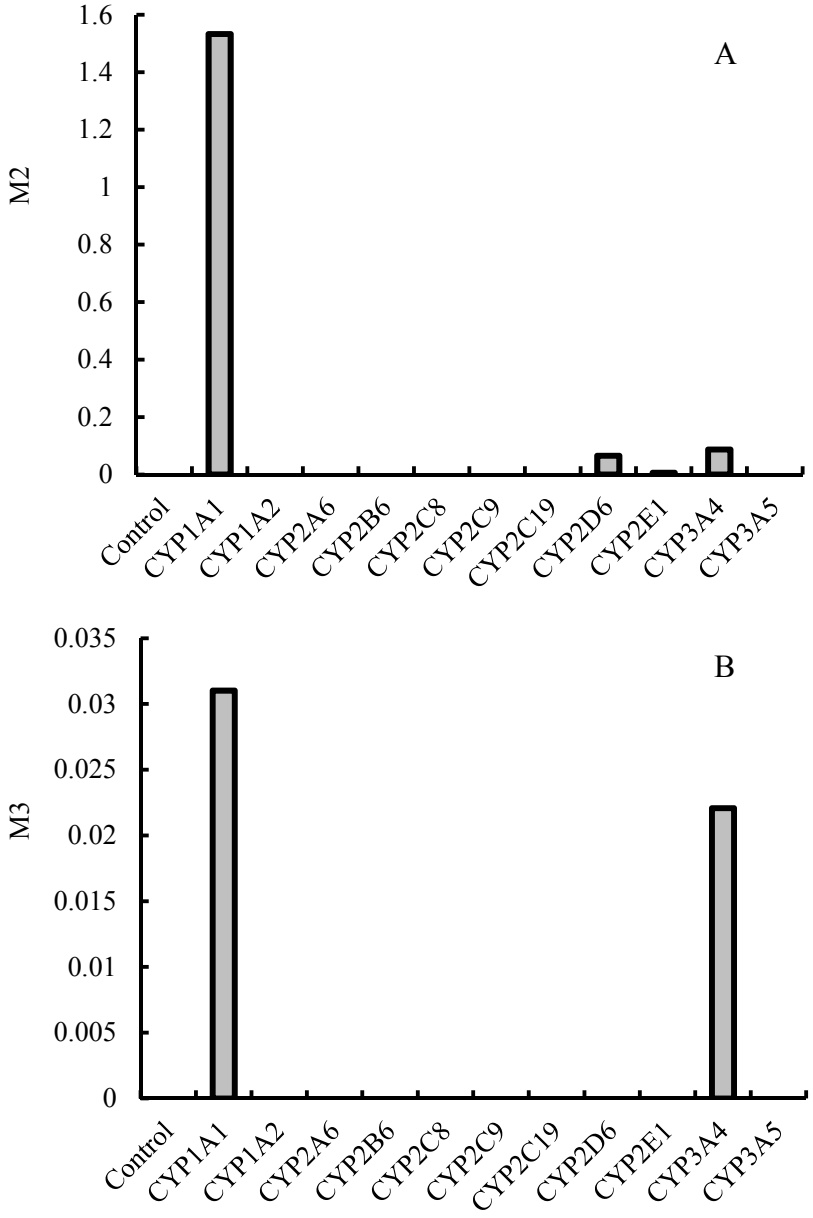

Fig. 2-5 Hydroxylation of M1 to M2 (A) and dehydrogenation of M2 to M3 (B) catalyzed by human CYP isozymes.

Recombinant CYP enzyme (50 nM) was assayed with 10 μM delamanid metabolite at 37°C for 30 min. The product was monitored by LC-MS/MS (mean peak area ratio of product to internal standard peak area, *n* = 2).

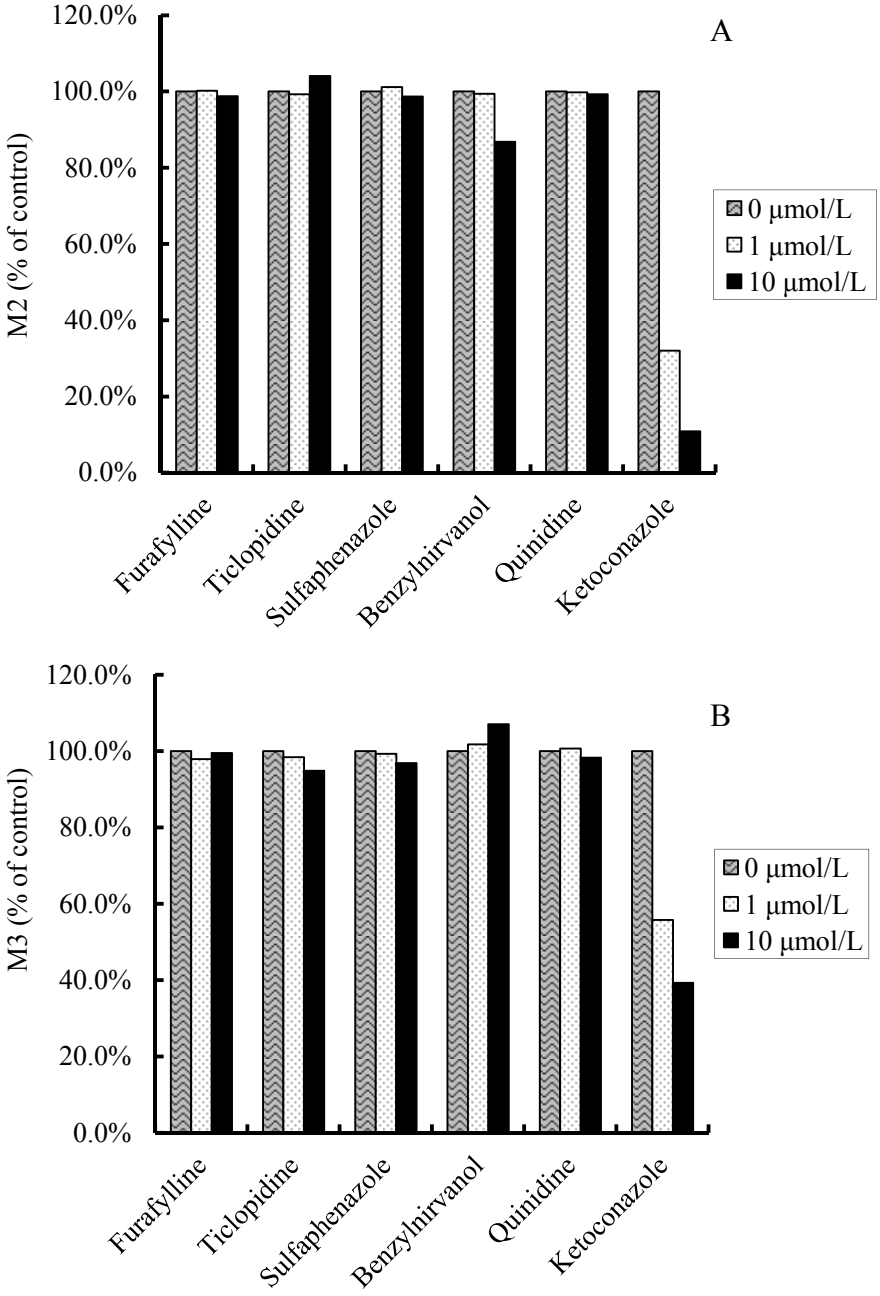

Fig. 2-6 Effects of various CYP inhibitors on hydroxylation of M1 (A) and dehydrogenation of M2 (B) in human liver microsomes.

Human liver microsomes (1 mg/mL) were assayed with 10 μM delamanid metabolite in the presence of a chemical inhibitor at 37°C. The product was measured by LC-MS/MS (mean, *n* = 2).

2.3.5. Binding of Metabolites to Serum

The *in vitro* protein binding of M1, M4, and M5 in mouse, rat, dog, and human sera is shown in Table 2-4. Calculation of protein binding for almost all metabolites at concentrations of 500 ng/mL was not performed because the metabolite levels in the buffer side were extremely low, which indicated high protein binding. At 5000 ng/mL, M1, M4, and M5 showed high protein binding (98.7%–99.8%). No differences in the metabolite intersubstrate and interspecies in addition to delamanid were observed.

Table 2-4 Protein binding of delamanid and metabolites in the mouse, rat, dog, and human.

Species	Concentration (ng/mL)	Protein binding (%)			
		Delamanid[a]	M1	M4	M5
Mouse	500	99.5	NC	NC	98.7
	5000	99.6	99.7	99.6	98.8
Rat	500	99.6	NC	NC	NC
	5000	99.6	99.4	99.7	98.9
Dog	500	99.5	NC	NC	NC
	5000	99.3	99.6	99.8	99.3
Human	500	99.5	NC	NC	NC
	5000	99.6	99.7	99.6	99.2

[a] Data were obtained from Chapter 3.
NC: not calculated (the concentration of the buffer side was below 6 ng/mL)
Values are the mean of *n* = 3.

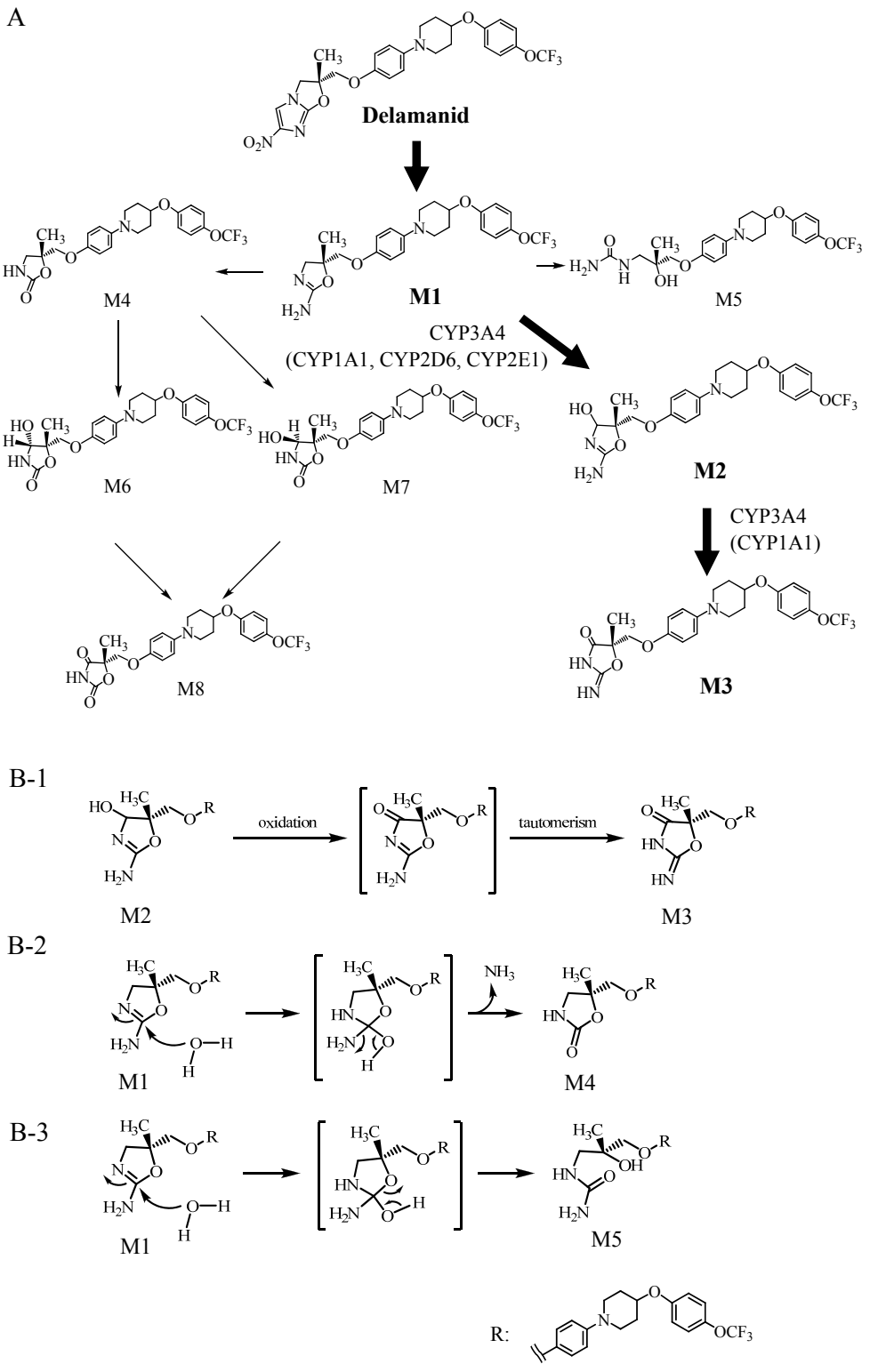

Fig. 2-7 Proposed metabolic pathways of delamanid (A) and metabolic mechanism of M2 to M3 (B-1), M1 to M4 (B-2), and M1 to M5 (B-3) in human.

Main reactions are symbolized by bold arrows. M1 to M3, M1 to M8, and M1 to M5 were defined as pathway 1, pathway 2, and pathway 3, respectively.

2.4. Discussion

Eight compounds were detected as circulating metabolites after repeated oral administration of delamanid in mice, rats, and dogs (Fig. 2-1). Drug-related peaks, except those for delamanid and its 8 metabolites, were not observed on UV chromatograms (Fig. 2-1B), which indicated that there were no other significant metabolites in the plasma. All metabolites had a common product ion at *m/z* 352 (Table 2-1), which is produced by the loss of the nitro-dihydro-imidazooxazole moiety of delamanid. Delamanid, M1, M2, M4, M5, M6, M7, and M8 gave the characteristic and intense product ions at *m/z* 357, 288, 302, 289, 306, 305, 305, and 303, respectively (Table 2-1), which were generated by the loss of the trifluoromethoxy phenol moiety. These results suggest that the nitro-dihydro-imidazooxazole moiety is the main metabolic target site of delamanid. An analog of delamanid, PA-824, which currently is being developed in a clinical trial for TB therapy, has a 2-nitro-imidazooxazine as well. PA-824 is metabolized mainly at the nitro-imidazole moiety in the liver (Dogra et al., 2011); hence, delamanid and PA-824 have a common metabolic target site, which suggests that this moiety has a position with high metabolic reactivity.

After consideration of our findings, we propose metabolic pathways of delamanid. In general, metabolic reactions, such as a monooxygenase reaction and hydrogen abstraction reaction, are simple. In contrast, metabolic reactions of delamanid and M1 are complicated. Since NADPH-dependent metabolites were hardly detected in human liver microsomes (Matsumoto et al., 2006), M1 was thought to be mainly produced from delamanid by extrahepatic mechanism. Moreover, all metabolites (M1 to M8) were detected in the animals following M1 administration (data not shown), which suggested that M1 is a crucial starting point of the metabolic pathway. In this study, following oral administration of delamanid to animals and humans, M1 to M8 were detected and identified in plasma. After considering

these findings, delamanid is thought to be primarily formed by hydrolytic cleavage of the hydroimidazo-oxazole moiety to (*R*)-2 amino-4,5-dihydrooxazole derivative (M1) and further catalyzed by 3 pathways (Fig. 2-7A). The first metabolic pathway (pathway 1) is hydroxylation of the oxazole moiety (M2) followed by oxidation of hydroxyl group and tautomerization of oxazole to an imino-ketone metabolite (M3, Fig. 2-7B-1). The second metabolic pathway (pathway 2) is hydrolysis and deamination of the oxazole amine (M4, Fig. 2-7B-2) followed by hydroxylation to M6 and M7 and oxidation of oxazole to another ketone metabolite (M8). The third metabolic pathway (pathway 3) is hydrolytic cleavage of the oxazole ring (M5, Fig. 2-7B-3).

After repeated administration of delamanid, the highest exposure in human subjects was to the parent compound (40% of the total exposure) followed by the metabolites M1 (18%) and M3 (13%) (Table 2-3). M1 showed the highest exposure among the 8 metabolites after repeated oral dosing in humans, which indicated that M1 is the predominant metabolite. The proposed major metabolic pathway of delamanid in humans is considered to be pathway 1. The exposures of M3 (17%), M1 (17%), M8 (13%), and M2 (12%) were high in the male dog plasma after repeated administration, which suggested that pathway 1 is the most important in dogs, followed by pathway 2. Conversely, exposure to M7 (4%–10%) was high in mice and rats, which suggested that pathway 2 is the most important in rodents. We consider that the metabolic pathways in dogs were similar to those in humans but dissimilar to those in rodents.

Qualitatively, the 8 metabolites were commonly observed in the animals and humans evaluated. However, there was a quantitative difference among the species (Table 2-3). The exposure ratios of the AUCs of all metabolites (M1–M8) to the total $AUC_{0\text{-}24h}$ were much higher in dogs (71%) and humans (60%) than in rodents (15%–18%), which indicated that dog metabolism is quantitatively similar to that of humans (Table 2-3). Regarding the species

differences, a larger amount of M1, which is a crucial starting point in the metabolic pathway, was generated in dogs and humans than in rodents (Table 2-3). This difference in M1 formation is likely to have a significant impact on the subsequent metabolism of delamanid.

Protein binding is an important factor regarding interspecies comparison of systemic exposure. Therefore, we determined plasma protein bindings of M1, M4, and M5 which are leading metabolites in each pathway. We found that there were no differences in the protein bindings of delamanid (Chapter 3) and these metabolites among mice, rats, dogs, and humans (Table 2-4). The presence or absence of correction for protein binding has limited effectiveness as long as interspecies comparison of systemic exposure is concern. The metabolites in humans were observed commonly in experimental animals; hence, the experimental animals could receive sufficient exposure to the metabolites by increasing the dose of delamanid. The interspecies pharmacokinetic profiles suggest that the animals were appropriately selected for the safety assessment of delamanid and its metabolites.

In humans, systemic exposure to delamanid after multiple oral dosing was 3.1 times higher than that after single administration, and a steady-state exposure was reached at 14 days (Fig. 2-4). In dogs like human, plasma levels of delamanid and also the metabolites increased during multiple dosing. In particular, the increases in M1, M2, M3, and M8 were extraordinarily large (Table 2-3). The accumulation is because of the extended half-lives ($t_{1/2,z}$: 108.0–884.2 h) of M1, M2, M3, and M8 (Fig. 2-2, Table 2-2). A possible explanation is that M1 distributes rapidly and becomes highly bound to many tissues. Because of the high affinity, moving back to the plasma compartment would be slow. This rapid tissue distribution and slow return to the plasma compartment may result in the extended half-lives in plasma. In fact, radioactive concentration in almost all tissues was higher than that in plasma following the administration of radiolabeled delamanid to rats (Miyamoto et al., 2005). Representative organs such as lung (target organ), liver and kidney showed high M1

ratio to total radioactivity, whereas M1 was seen at a very low level in the plasma. Therefore, many tissues exhibited an extremely high distribution of M1 compared with the plasma. Moreover, M1 is likely oxidized after liver uptake, and the oxidized metabolites are returned more slowly to the plasma compartment.

We also carefully examined the activities of CYP isoforms involved in pathway 1, the major metabolic pathway in humans. The *in vitro* metabolism of M1 and its oxide (M2) was investigated using human recombinant CYP isoforms. Recombinant CYP1A1 and CYP3A4 converted these compounds to the oxidized metabolite, but other recombinant CYPs had little metabolic activity (Fig. 2-5). Furthermore, we investigated the inhibition of formation of metabolites using CYP chemical inhibitors in human liver microsomes. Ketoconazole, a CYP3A4 inhibitor, decreased hydroxylation of M1 to M2 and oxidation of M2 to M3 in human liver microsomes in a concentration-dependent manner, whereas the other chemical inhibitors for other CYPs did not show any appreciable degree of inhibition (Fig. 2-6). On the basis of these studies, CYP3A4 is considered to be the major CYP isoform responsible for M2 and M3 formations. In addition, CYP3A4 was responsible for the reactions that formed M7 from M4 and M8 from M6 in the liver (data not shown), which involve similar hydroxylation and oxidation of the oxazole moiety. Conversely, CYP1A1 is not presumed to be principally involved in the metabolism because of the extremely low amounts of CYP1A1 in the human liver (Schweikl et al., 1993; Imaoka et al., 1996). Therefore, CYP3A4 was thought to play an important role in the overall metabolism from M1. Nevertheless, we consider that delamanid and the key metabolite, M1, are less affected by inhibitor CYPs, probably because the metabolism of delamanid to M1 is due to a nonhepatic process, and M1 has multiple metabolic pathways. No significant changes in delamanid and M1 exposure occurred when delamanid was co-administered with lopinavir/ritonavir, a CYP3A4 inhibitor (Paccaly et al., 2012). Furthermore, delamanid is not affected by efavirenz, a CYP3A4

inducer (Petersen et al., 2012). On the other hand, PA-824 exposures are substantially reduced by concomitant efavirenz while lopinavir/ritonavir had minimal effect on PA-824 exposures (Dooley et al., 2014). These findings suggest that even though extrahepatic metabolism may occur with PA-824, the contribution of extrahepatic metabolism on PA-824 is lower than that for delamanid. These metabolic features of delamanid are a key point of differentiation from many other drugs, which are catalyzed mainly by CYPs.

In conclusion, delamanid is primarily degraded to M1 by extrahepatic mechanism and further catalyzed by 3 metabolic pathways, which indicates that M1 is a crucial starting point. M1 had the highest exposure among the 8 metabolites detected after repeated oral dosing in humans. M1 was subsequently oxidized to M3 via M2 mainly by CYP3A4. The pharmacokinetics and overall metabolism of delamanid show species differences, which are probably caused by the activity of extrahepatic metabolism on delamanid. We concluded that M1 formation caused by the metabolism is the most important contributor to the pharmacokinetics and metabolism of delamanid. Clinically significant drug–drug interactions (DDIs) of delamanid and M1 with other drugs are considered to be limited.

2.5. Chapter summary

In this study, we characterized the pharmacokinetics and metabolism of delamanid in animals and humans. Eight metabolites (M1 to M8) produced cleavage of the imidazooxazole moiety of delamanid were identified in the plasma after repeated oral administration by LC-MS/MS analysis. Delamanid was initially catalyzed to M1 and subsequently metabolized by 3 separate pathways, which suggested that M1 is a crucial starting point. The major pathway in humans was hydroxylation of the oxazole moiety of M1 to form M2 and then successive oxidation to the ketone form (M3) mainly by CYP3A4. M1 had the highest exposure among the 8 metabolites after repeated oral dosing in humans, which indicated that M1 was the major metabolite. The overall metabolism of delamanid was qualitatively similar across nonclinical species and humans, but quantitatively different among the species. After repeated administration, the metabolites had much higher concentrations in dogs and humans than in rodents. Nonhepatic formation of M1 and multiple separate pathways for metabolism of M1 suggest that clinically significant DDIs with delamanid and M1 are limited.

Chapter 3

In Vitro Metabolism of Delamanid in Animal and Human Plasma

3.1. Objectives

When delamanid was incubated with liver microsomes in the presence of NADPH, metabolites were not detected in the reaction mixture, suggesting that delamanid was not metabolized by CYP enzymes (Matsumoto et al., 2006). However, the major metabolite (*R*)-2-amino-4,5-dihydrooxazole derivative (M1) in human and animal plasma were detected and identified in the investigation for the *in vivo* pharmacokinetics and metabolism of delamanid, as described in Chapter 2. On the basis of the chemical structure of M1, it is proposed that delamanid is cleaved directly at its 6-nitro-2,3-dihydro-imidazo[2,1-*b*]oxazole moiety by some extrahepatic mechanism (Matsumoto et al., 2006).

It is important to identify the enzymes responsible for the metabolism of delamanid in humans. In the current study, biotransformation was first examined in animal and human plasma, and then the metabolic byproduct was identified by detection of radioactivity and simultaneous mass spectrometry (MS). The effects of temperature and pH on the formation of M1 and the rates of delamanid metabolism by various plasma protein fractions isolated by ultrafiltration and gel filtration were also investigated to identify the responsible enzymes. Finally, the kinetic parameters of M1 production were compared between human plasma and specific plasma proteins, which identified albumin as a major mediator of delamanid degradation. This is the first report describing the *in vitro* mechanism of delamanid metabolism in plasma.

3.2. Materials and Methods

3.2.1. Materials

^{14}C-Delamanid, delamanid, and its metabolite M1 were obtained from Otsuka Pharmaceutical Co., Ltd. The chemical structure and labeled position of ^{14}C-delamanid are shown in Fig. 3-1. The specific radioactivity of ^{14}C-delamanid was 4.14 MBq/mg, and the radiochemical purity was 99.2% as determined by high-performance liquid chromatography (HPLC).

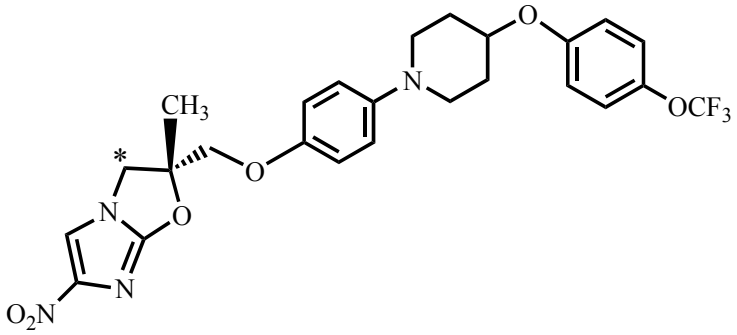

Fig. 3-1 Chemical structure of ^{14}C-delamanid.

Asterisk denotes the position of ^{14}C-radiolabel.

Human plasma using heparin as anticoagulant and human serum were prepared from three healthy males with approval of the Institutional Ethics Committee. Heparin plasma and serum from male mouse (ICR), rat (SD), rabbit (New Zealand White), and dog (beagle) were supplied by Kitayama Labes Co. These animals were used as the preclinical species in pharmacology, pharmacokinetics, and toxicology studies for delamanid. Purified human serum albumin (HSA), essentially fatty acid free prepared from serum Fraction V (product no A1887), rat serum albumin from Fraction V (RSA, A6272), canine serum albumin from Fraction V [dog serum albumin (DSA), A9263], human γ-globulin (G4386), and α_1-acid glycoprotein [(AGP), G9885] were purchased from Sigma-Aldrich Co. Other reagents were commercially available and of analytical grade.

3.2.2. Metabolism of Delamanid in Plasma

^{14}C-Delamanid was dissolved in methanol at 2.07 MBq/0.5 mg/mL. The reaction mixture consisted of ^{14}C-delamanid (5 μg/mL, 9.3 μM) and mouse, rat, rabbit, dog, or human plasma. The final solvent concentration was 1% (v/v). After preincubation of plasma at 37°C for 3 min, the reaction was started by adding ^{14}C-delamanid (5 μg/mL). Incubation at 37°C was continued for 0, 0.5, 1, 2, and 4 h. Non-labeled delamanid (50 μg/mL) was also incubated at 37°C for 24 h in mouse plasma to investigate the molecular structure of metabolites by MS.

3.2.3. Effects of Temperature and pH on Metabolite Formation in Plasma

^{14}C-Delamanid (5 μg/mL) in human plasma was incubated at 25°C and 0°C for 0, 1, 2, and 4 h (in addition to at 37°C for 0, 0.5, 1, 2, and 4 h). Further, ^{14}C-delamanid (5 μg/mL) was incubated at 37°C for 0, 0.5, 1, 2, and 4 h in 50 mM phosphate buffer (pH 6.0, 7.0, 7.5, and 8.0) containing 10% human plasma.

3.2.4. Metabolite Formation in Fractionated Plasma

Human plasma was centrifuged at 3000 g for 30 min using a Centricon YM-30 (molecular mass cutoff of 30 kDa, Millipore Co.). The plasma filtrate was incubated with ^{14}C-delamanid (5 μg/mL) at 37°C for 0, 0.5, 1, 2, and 4 h.

To obtain plasma protein fractions, high-performance gel filtration chromatography of human plasma was performed at room temperature using the columns TSK-gel G4000SW$_{XL}$ (7.8 mm ID × 300 mm, 8 μm particle size, Tosoh Co.) and TSK-gel

$G3000SW_{XL}$ (7.8 mm ID × 300 mm, 5 μm particle size, Tosoh Co.) in combination, 50 mM phosphate buffer (pH 7.0) as the mobile phase at 1 mL/min, and UV detection at 280 nm. After injection of 200 μL human plasma, the effluent was fractionated every 1 min. Pure HSA (40 mg/mL), γ-globulin (12 mg/mL), and AGP (1 mg/mL) were also analyzed to confirm retention times. The eluate was adjusted to pH 7.5 with 1N sodium hydroxide and incubated with 5 μg/mL of ^{14}C-delamanid at 37°C for 8 h. Delamanid was also incubated with HSA (40 mg/mL), γ-globulin (12 mg/mL), or AGP (1 mg/mL) in place of the eluate fraction containing all three proteins.

3.2.5. Kinetic Analysis on Metabolite Formation in Plasma and Human Serum Albumin

^{14}C-Delamanid [10, 25, 50, 100, 250, and 500 μM in 2% dimethyl sulfoxide (DMSO)] was incubated at 37°C for 0.25 h in human plasma or 40 mg/mL HSA (both in 50 mM phosphate buffer, pH 7.4). Total plasma protein concentration was determined using a Bio-Rad DC protein assay kit.

3.2.6. Metabolite Profiling in Plasma and Albumin

^{14}C-Delamanid (5 μg/mL) was incubated in 50 mM phosphate buffer (pH 7.4) containing either 50% plasma or 20 mg/mL albumin from rat, dog, and human at 37°C for 0, 0.5, 1, and 2 h.

3.2.7. Binding of Delamanid to Serum and Human Serum Albumin

Degradation of delamanid is temperature-dependent. To avoid the degradation of

delamanid, the protein binding studies were conducted at 20°C. The *in vitro* binding of ^{14}C-delamanid (0.05, 0.5, and 5 μg/mL) to animal and human serum was determined by equilibrium dialysis for 4 h (rabbit and dog serum) or 8 h (rat, mouse, and human serum) using Spectra/Por2 molecular porous dialysis membrane (Spectrum Laboratories, Inc.). The binding of ^{14}C-delamanid (0.05, 0.5, and 5 μg/mL) to RSA, DSA, and HSA solutions (all at 40 mg/mL) was also determined. Further, the binding of ^{14}C-delamanid (3 μM) to HSA (15 μM, 1 mg/mL) was determined in the absence and presence of the site-specific HSA binding probes warfarin (Site I), diazepam (Site II), and digitoxin (Site III), all at 15, 75, and 150 μM. DMSO content was always ≤1% (v/v). The dialyzed protein and dialysate were analyzed to determine the delamanid concentrations in bound and unbound fractions. After a scintillator cocktail was added to the sample, the radioactivity was determined by a liquid scintillation counter (LSC-3500, Aloka Co.).

3.2.8. Sample Preparation for Radioactivity Counting and Mass Spectrometry

The reaction was terminated by mixing with 2 volumes of acetonitrile-formic acid (90:10, v/v). Following centrifugation at 21800 *g* for 5 min, 30 μL of the supernatant was analyzed by HPLC with simultaneous radioactive detection. Further, a scintillator cocktail (ACS II, Amersham Bioscience UK Ltd.) was added to 30 μL of the supernatant, and the radioactivity determined by liquid scintillation (LSC-3500) to evaluate extraction and column recovery.

For measuring the metabolism of unlabeled delamanid in plasma, the reaction was terminated by mixing in an equal amount of acetonitrile, followed by centrifugation at 21800 *g* for 5 min and LC-MS/MS.

3.2.9. High-Performance Liquid Chromatography and Liquid Chromatography-Tandem Mass Spectrometry Procedures

To investigate the metabolism of labeled delamanid in plasma, two HPLC protocols were used. HPLC Method 1 utilized a LC-10A HPLC system (Shimadzu Co.) equipped with a TSK-gel ODS-80Ts QA C18 column (4.6 mm ID × 150 mm, 5 μm particle size, Tosoh Co.) for sample analysis. The analyte was separated using a binary solvent linear gradient with mobile phase A [water–acetic acid (100:1, v/v)] and B [acetonitrile –acetic acid (100:1, v/v)]; 0% B to 60% B from 0 to 35 min; 60% B to 90% B from 35 to 40 min at a flow rate of 1 mL/min, isocratic elution at 90% B from 40 to 45 min, and 0% B from 45 to 60 min. Before entering the radioactive flow detector, the column effluent was mixed in-flow with 1:2 scintillation cocktail (Ultima-Flo AP, PerkinElmer, Inc.) pumped at a rate of 2 mL/min. The radioactivity in the effluent was monitored using a Radiomatic 525TR flow scintillation analyzer (PerkinElmer, Inc.). In HPLC Method 2 used to investigate the effects of temperature and pH, metabolite formation, kinetic analysis, and metabolite profiling in plasma and albumin were conducted using a model 2695 Alliance HPLC system (Waters Co.) equipped with a TSK-gel ODS-80Ts QA C18 column. The elution was performed using a binary solvent linear gradient from 30% B to 90% B from 0 to 15 min at a flow rate of 1 mL/min, 30% B from 15 to 20 min at 1.2 mL/min, and 30% B from 20 to 25 min at a flow rate of 1 mL/min. The radioactivity in the effluent was monitored using a flow scintillation analyzer.

To investigate the metabolism of unlabeled delamanid in plasma, delamanid and metabolite were analyzed by the LC-MS/MS method, as described in Chapter 2.2.3.

3.2.10. Data Processing

Data processing was performed using FLO-ONE version 3.65 (PerkinElmer, Inc.) in the flow scintillation analyzer. The radioactivity of delamanid metabolite in the sample was determined on the radiochromatogram, and the radioactivity was converted to equivalents of delamanid. The residual content of delamanid, metabolite formation, and other calculations were conducted with Microsoft Excel version 2003. The half-life and Michaelis–Menten parameters [Michaelis–Menten constant (K_m) and maximum velocity (V_{max})] were calculated using a nonlinear least squares method by WinNonlin version 5.2 (Pharsight Co.). The intrinsic clearance (CL_{int}) was obtained from V_{max}/K_m. Analysis of LC-MS/MS was performed using Analyst version 1.4.2 (AB SCIEX).

3.3. Results

3.3.1. Metabolism of Delamanid in Plasma

The degradation of ^{14}C-delamanid during incubation in plasma at 37°C is shown in Fig. 3-2 and Table 3-1. Delamanid was rapidly degraded by incubation in human, dog, rabbit, mouse, or rat plasma at 37°C, with shortest half-life in human plasma (0.64 h), followed by dog (0.84 h), rabbit (0.87 h), mouse (1.90 h), and rat (3.54 h).

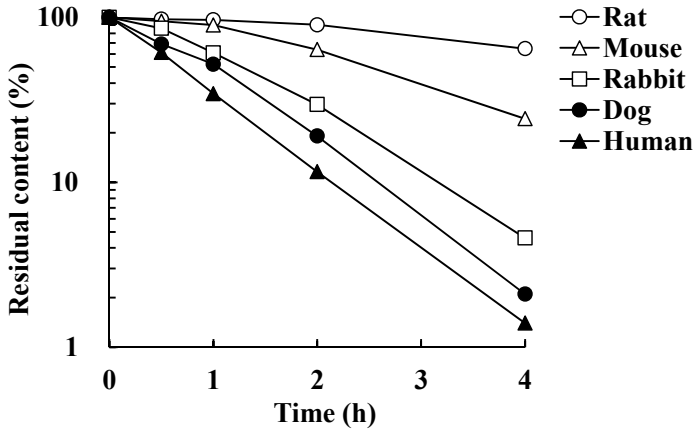

Fig. 3-2 Stability of delamanid in animal and human plasma *in vitro*.

^{14}C-Delamanid (5 μg/mL, 9.3 μM) was incubated in rat, mouse, rabbit, dog, or human plasma at 37°C. Data points are the means of duplicate determinations.

Table 3-1 *In vitro* disappearance of delamanid in plasma of different species.

Species	Half-life (h)
Rat	3.54
Mouse	1.90
Rabbit	0.87
Dog	0.84
Human	0.64

^{14}C-Delamanid (5 μg/mL) was incubated with plasma at 37°C in duplicate determinations.

Typical HPLC radiochromatograms of delamanid metabolites in plasma are shown in Fig. 3-3. The major delamanid byproduct, M1, increased as substrate concentration decreased in plasma samples from all species.

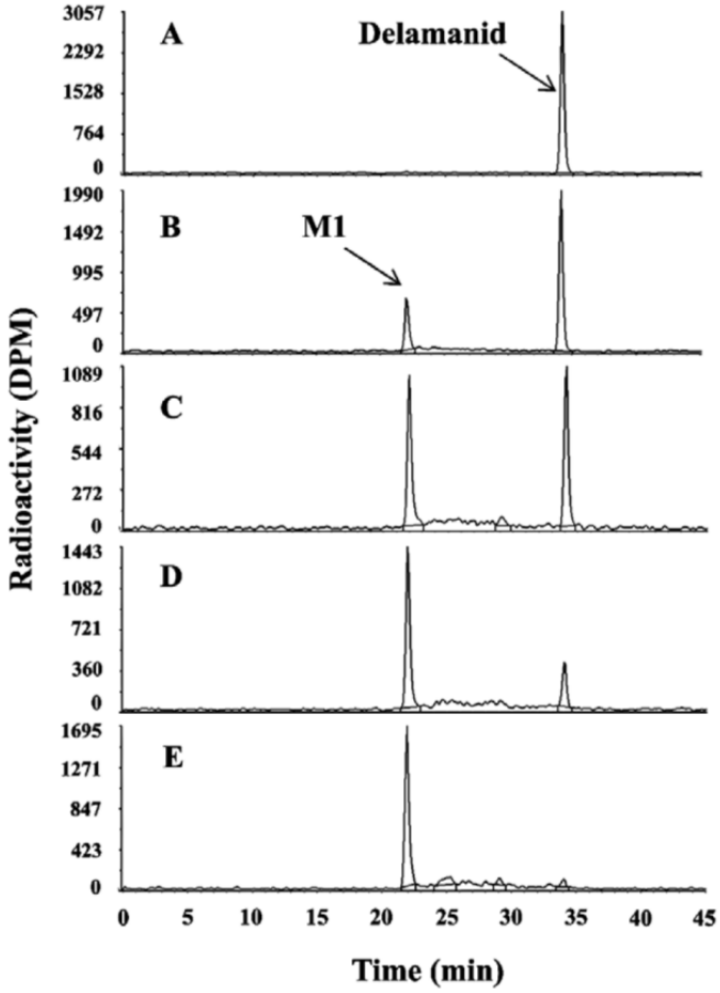

Fig. 3-3 HPLC radiochromatograms of delamanid metabolites in human plasma.

^{14}C-Delamanid (5 μg/mL) was incubated at 37°C for 0 h (A), 0.5 h (B), 1 h (C), 2 h (D), and 4 h (E) in human plasma.

The chemical structure of M1 was further investigated by LC-MS/MS analysis of mouse plasma containing non-labeled delamanid. The mass spectra of the parent compound and the metabolite revealed protonated molecules ($[M+H]^+$) at *m/z* 535 and 466, respectively, and a characteristic and intense fragment ion at *m/z* 352 in both positive product ion spectra (Fig. 3-4). The peak profile of the metabolite indicated the existence of a 4-[4-(4-trifluoro-methoxyphenoxy)piperidin-1-yl]phenoxy moiety without imidazooxazole. Additional fragment ions were observed at *m/z* 357 in spectra of the parent drug and at *m/z*

113, 288, and 449 in spectra of the metabolite. The metabolite M1 was identified as (*R*)-2-amino-4,5-dihydrooxazole derivative by comparing the mass spectra and retention time of the product in the plasma sample to those of the authentic standard.

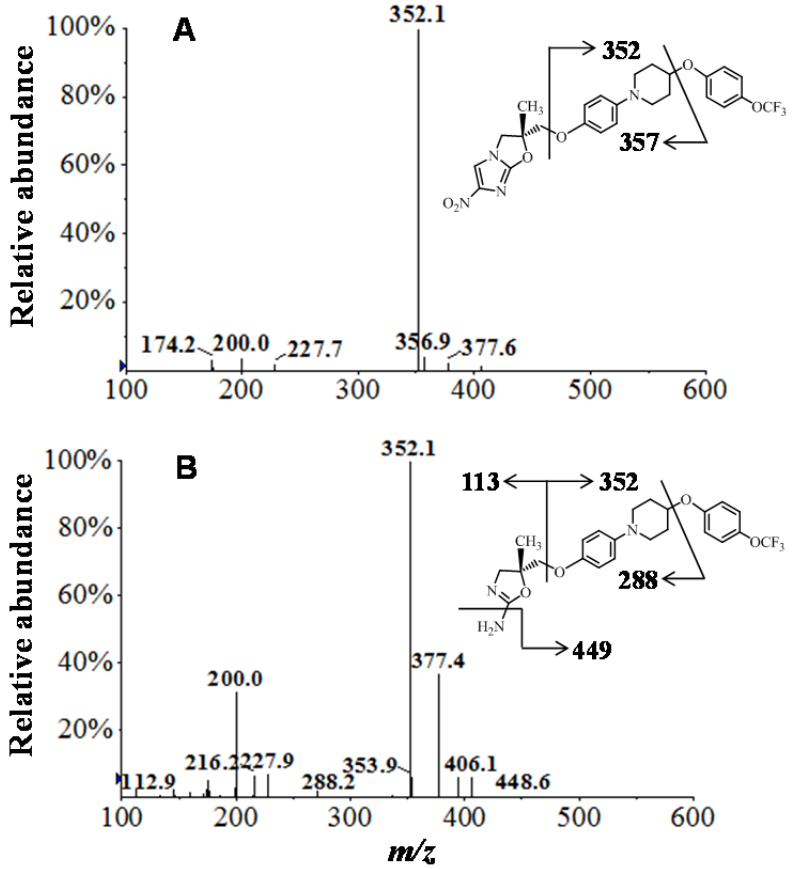

Fig. 3-4 Product ion spectra of delamanid at *m/z* 535 (A) and M1 at *m/z* 466 (B).

The product was investigated by LC-MS/MS following incubation of delamanid in mouse plasma at 37°C.

3.3.2. Effects of Temperature and pH on Metabolite Formation in Plasma

The rates of M1 formation in human plasma incubated at various temperatures are shown in Fig. 3-5. The biotransformation to M1 after 4 h was 51.7% at 37°C and 36.3% at

25°C, whereas no M1 was detected after 4 h at 0°C.

Metabolism was also highly pH-dependent (Fig. 3-6). After 4 h at 37°C in 10% human plasma, M1 formation was 0.0% at pH 6.0, 4.8% at pH 7.0, 12.7% at pH 7.5, and 20.1% at pH 8.0. In contrast, M1 was not formed during incubation for 4 h in 50 mM phosphate buffer at any pH in the absence of plasma (data not shown).

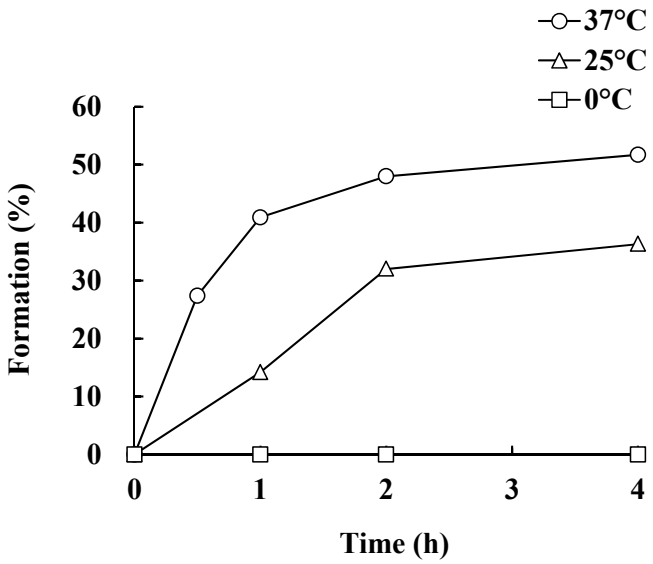

Fig. 3-5 Temperature dependence of M1 formation from delamanid in human plasma.

^{14}C-Delamanid (5 μg/mL) was incubated in human plasma.

Data points are the means of duplicate determinations.

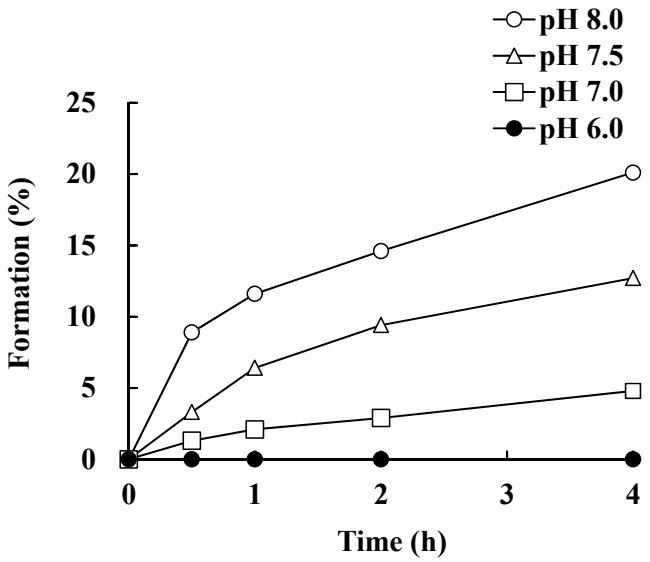

Fig. 3-6 The pH dependence of M1 formation from delamanid in human plasma. **^{14}C-Delamanid (5 μg/mL) was incubated in a solution of 10% plasma and 50 mM phosphate buffer (balance to the indicated pH) at 37°C. Data points are the means of duplicate determinations.**

3.3.3. Metabolite Formation in Fractionated Plasma

Delamanid was not converted to M1 in the filtrate of human plasma obtained with a molecular mass cutoff of 30 kDa, indicating that metabolism required the presence of plasma proteins of molecular mass ≥30 kDa. When delamanid degradation was examined in plasma fractions separated by gel chromatography, M1 was observed in the fraction containing albumin, γ-globulin, and AGP (Fig. 3-7). In the presence of HSA, delamanid was metabolized to M1, whereas no M1 was detected following delamanid incubation with γ-globulin or AGP (data not shown). Thus, metabolism requires HSA.

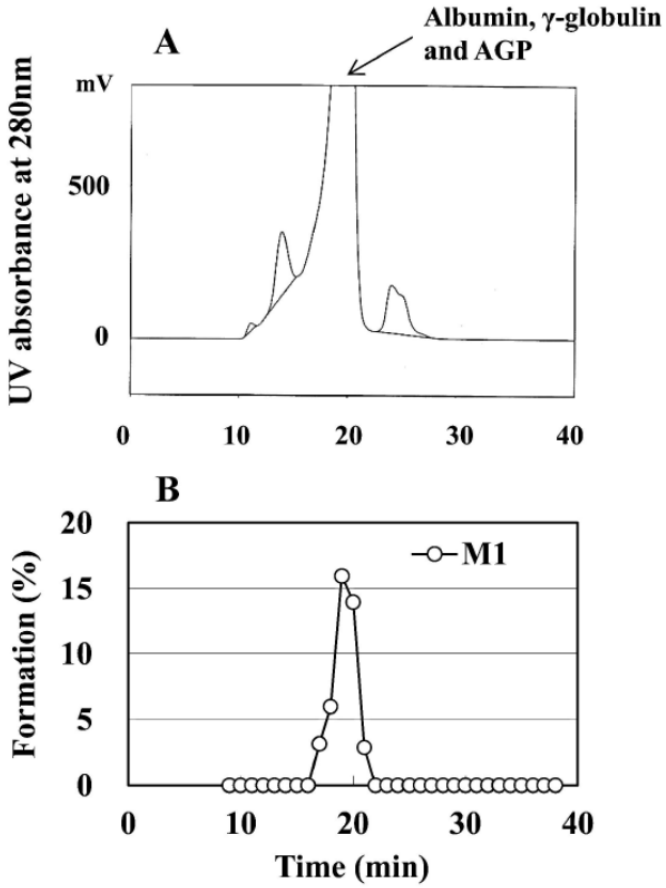

Fig. 3-7 M1 formation from delamanid in human plasma fractions separated by gel filtration chromatography.

(A): After 200 μL of human plasma was injected into the high-performance gel filtration chromatography system, the effluent was fractionated every 1 min. Authentic human albumin, γ-globulin, and AGP were also run.

(B): ^{14}C-Delamanid (5 μg/mL) was incubated in the human plasma fractions at 37°C for 8 h.

3.3.4. Kinetic Analysis on Metabolite Formation in Plasma and Human Serum Albumin

The total protein concentration in human plasma samples was approximately 80 mg/mL. Several concentrations of delamanid were incubated in human plasma or 40 mg/mL HSA. The formation of M1 followed Michaelis–Menten kinetics in both human plasma and HSA (Fig. 3-8). The Eadie–Hofstee plot for the formation of M1 in plasma showed a monophasic profile. The K_m, V_{max}, and CL_{int} values for plasma were 67.8 μM, 7.55 pmol/min/mg, and 0.111 μL/min/mg, respectively, and the values found in HSA alone, which were 51.5 μM, 11.7 pmol/min/mg, and 0.227 μL/min/mg (Table 3-2).

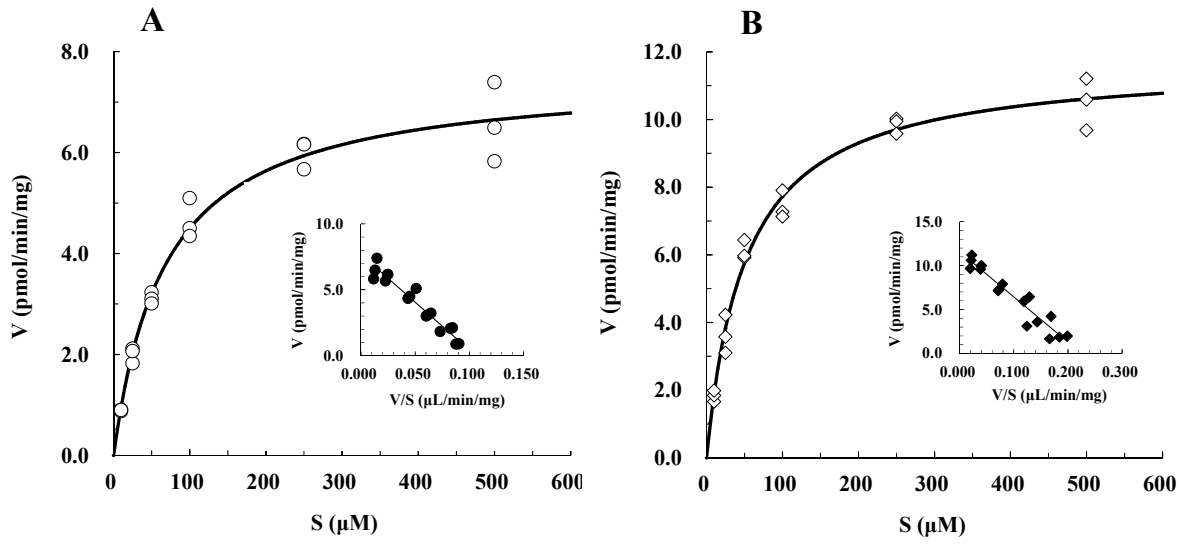

Fig. 3-8 Michaelis–Menten and Eadie–Hofstee plots for M1 formation in human plasma and HSA.

^{14}C-Delamanid (10 to 500 μM) was incubated in a solution of human plasma (A) or 40 mg/mL HSA (B) with 50 mM phosphate buffer (pH 7.4) at 37°C for 0.25 h. S is the substrate concentration of delamanid and V is the velocity of M1 formation. Insets are the corresponding Eadie–Hofstee plots. Data points are the means of triplicate determinations.

Table 3-2 Kinetic parameters for M1 formation in human plasma and HSA.

Protein	K_m (μM)	V_{max} (pmol/min/mg)	CL_{int} (μL/min/mg)
Human plasma	67.8	7.55	0.111
HSA	51.5	11.7	0.227

^{14}C-Delamanid (10 to 500 μM) was incubated in human plasma or 40 mg/mL HSA at 37°C for 0.25 h. M1 formation was determined by radio-HPLC analysis. Each value was calculated using the mean formation data of triplicate determinations.

3.3.5. Metabolite Profiling in Plasma and Albumin

In addition to the kinetic profile, the metabolic pattern of delamanid in 50% plasma was similar to that in 20 mg/mL albumin (Fig. 3-9). The degradation rates of delamanid were highest in human plasma and HSA, followed by dog and rat plasma and albumin. The residual content of delamanid after 1 h at 37°C in 50% human plasma was 52.8%, substantially higher than in dog (82.6%) and rat (93.5%), whereas the corresponding biotransformation rate to M1 was highest in 50% human plasma (21.0%), followed by dog (6.5%) and rat (3.1%). Similarly, the residual delamanid content was lower after incubation (1 h at 37°C) in 20 mg/mL HSA (50.1%) compared with that in DSA (77%) and RSA (92.0%), and corresponding M1 formation was highest in HSA (19.9%), followed by DSA (9.7%) and RSA (5.2%).

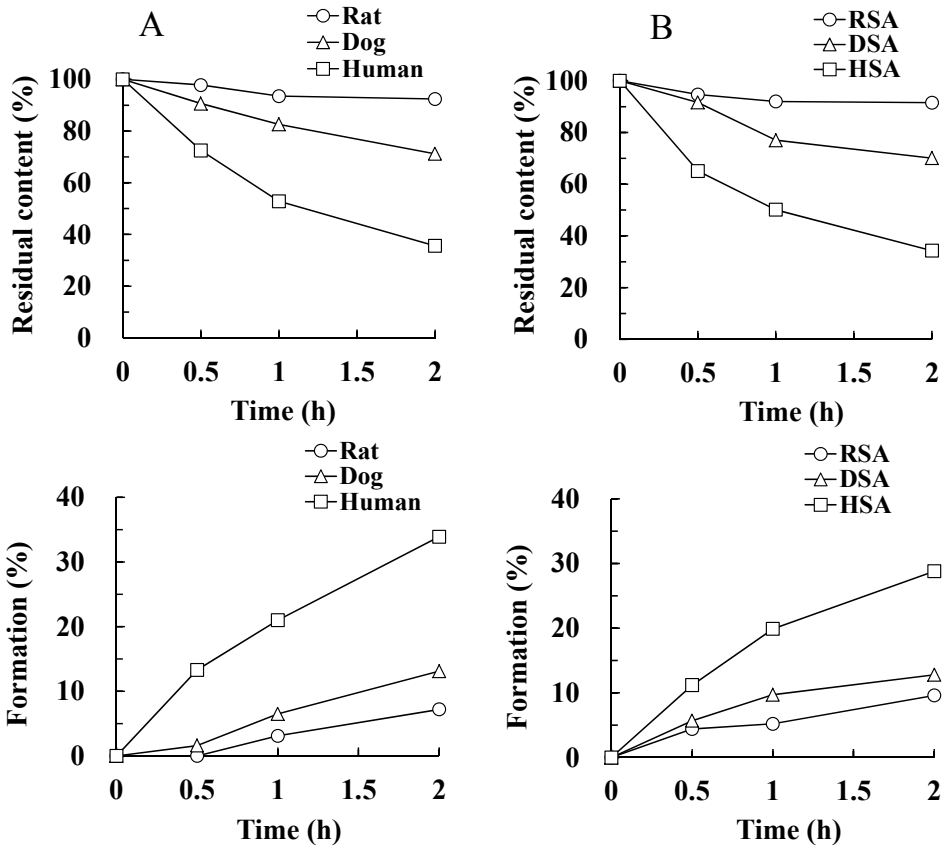

Fig. 3-9 Degradation of delamanid and M1 production in diluted plasma (A) and albumin (B) from rat, dog, and human.

^{14}C-Delamanid (5 μg/mL) was incubated in 50% plasma or 20 mg/mL albumin (both in 50 mM phosphate buffer, pH 7.4) at 37°C. Data points are the means of duplicate determinations.

3.3.6. Binding of Delamanid to Serum and Human Serum Albumin

The *in vitro* protein binding ratio was ≥99.3% in all serum samples at all ^{14}C-delamanid concentrations tested (Table 3-3), while binding was ≥97.4% to RSA, DSA, and HSA. The binding of ^{14}C-delamanid to HSA was not changed in the presence of the Site I-specific binding probe warfarin, the Site II-specific probe diazepam, or the Site III-specific probe digitoxin (Table 3-4). The radiochemical purity of delamanid incubated at 20°C in

human serum and HSA was more than 86%, suggesting that delamanid was stable in the protein binding studies.

Table 3-3 *In vitro* binding of delamanid to serum and albumin.

Protein	Protein binding (%)		
	0.05 μg/mL	0.5 μg/mL	5 μg/mL
Rat serum	NT	99.6 ± 0.0	99.6 ± 0.0
Mouse serum	NT	99.5 ± 0.0	99.6 ± 0.0
Rabbit serum	NT	99.5 ± 0.0	99.5 ± 0.0
Dog serum	NT	99.5 ± 0.0	99.3 ± 0.2
Human serum	NT	99.5 ± 0.0	99.6 ± 0.0
RSA	98.5 ± 0.1	98.9 ± 0.0	98.9 ± 0.0
DSA	97.6 ± 0.1	98.1 ± 0.0	98.3 ± 0.0
HSA	97.4 ± 0.3	98.4 ± 0.1	98.5 ± 0.1

Equilibrium dialysis was performed at 20°C in serum or 40 mg/mL albumin (both spiked with ^{14}C-delamanid). NT = Not Determined.

Data are mean ± S.D. of triplicate determinations.

Table 3-4 Effects of warfarin, diazepam, and digitoxin on delamanid binding to HSA.

Probe	Probe concentration (μM)	Delamanid protein binding (%)
Control	0	98.7 ± 0.1
Warfarin	15	98.6 ± 0.2
	75	98.5 ± 0.1
	150	98.5 ± 0.2
Diazepam	15	98.6 ± 0.2
	75	98.6 ± 0.2
	150	98.7 ± 0.1
Digitoxin	15	98.2 ± 0.3
	75	97.8 ± 0.5
	150	98.0 ± 0.4

Equilibrium dialysis was performed for 6 h at 20°C in 15 μM (1 mg/mL) HSA spiked with ^{14}C-delamanid (3 μM) in the absence or presence of the protein binding probe.

Data are mean ± S.D. of four determinations.

3.4. Discussion

When delamanid was incubated in human plasma at appropriate temperature and pH, the metabolite M1 increased in parallel with a decrease in the substrate concentration, indicating that M1 is a primary produce of plasma-mediated degradation. M1 was also the most abundant primary metabolite detected during incubation in human plasma, as well as in plasma from other species. Degradation of delamanid was temperature-dependent, pH-dependent, saturable, and followed Michaelis–Menten kinetics. The Eadie–Hofstee plot for M1 formation was monophasic (Fig. 3-8), suggesting that the formation is catalyzed by one enzyme. Further, the formation of M1 in HSA followed Michaelis–Menten kinetics, with a K_m value similar to that in human plasma (Table 3-2), suggesting that plasma albumin, which constitutes about half of total plasma protein (40 mg/mL of 80 mg/mL), is likely responsible for the metabolism of delamanid. The V_{max} and CL_{int} values for delamanid in plasma (7.55 pmol/min/mg and 0.111 μL/min/mg), were comparable to those in 40 mg/mL HSA (11.7 pmol/min/mg and 0.227 μL/min/mg of albumin). In contrast, no delamanid metabolism was observed following incubation with the other two high molecular weight proteins, γ-globulin and AGP (data not shown). The purity of the commercial albumin employed in the *in vitro* studies was >96%, with the remainder being mostly globulins (Sigma, quality A-1887). Though hydrolase (mainly pseudo-cholinesterase) contamination of the purified HSA preparation cannot be completely excluded, metabolism was also observed by recombinant human albumin (product no A7223, Sigma-Aldrich Co.). This result and the similarity in kinetics between HSA and plasma strongly suggest that delamanid is metabolized predominantly by albumin in plasma.

The *in vitro* biotransformation of delamanid increased in a pH-dependent manner

(Fig. 3-6), and delamanid did not degrade at pH 6.0. Considering that pKa of delamanid is approximately 4.3, the pH sensitivity suggests that the pKa value of the catalytic amino acid residue(s) in plasma albumin may be important for the reaction. The metabolic patterns of delamanid in dog and rat plasma were also similar to those in dog and rat albumin (Fig. 3-9), suggesting that plasma albumin is predominantly responsible for delamanid metabolism in rat and dog as well. Protein binding to delamanid was also similar to that in humans (Table 3-3). Nonetheless, the degradation rate of delamanid was highest in human plasma and albumin solution, followed by dog and rat. It was reported that the hydrolytic degradation of Boc5 in plasma was mediated by serum albumin, and that species differences in hydrolysis could be attributed to variations in albumin sequence and high-order structure across species (Ge et al., 2013). The species differences in the degradation rate of delamanid may thus also stem from species variation in the sequence of albumin.

Though extraction recovery and HPLC column recovery were favorable, the rate of delamanid degradation was higher than the rate of M1 formation in both plasma and albumin, suggesting that M1 is the major but not the only metabolic byproduct. These other byproducts may include the minor metabolites observed at retention times from 24 to 30 min (Fig. 3-3), which remain to be identified and characterized.

In a novel biotransformation, M1 was uniquely formed by cleavage of the 6-nitro-2,3-dihydroimidazo[2,1-*b*]oxazole moiety of delamanid in plasma albumin. On the basis of the fact that the authentic standard M1 is directly synthesized from delamanid and alkaline reagents such as 25% ammonia solution or alkylamines, basic amino acid residues such as lysine or arginine in albumin may be important for the metabolism of delamanid. The proposed degradation mechanism of delamanid by albumin is illustrated in Fig. 3-10.

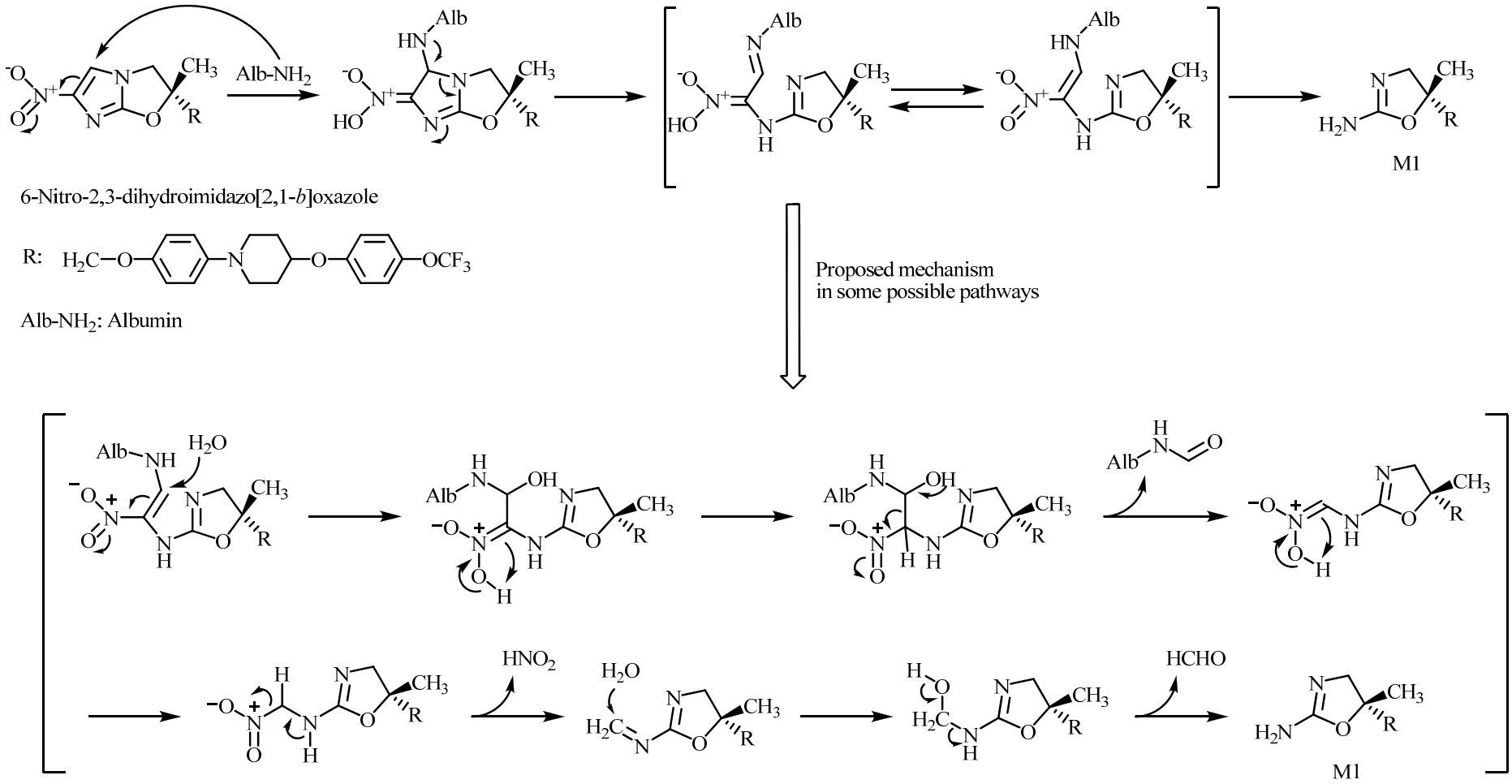

Fig. 3-10 Proposed degradation mechanism of delamanid by albumin.

Because of the electron withdrawing property of the neighboring nitro group, the electron-poor C-5 of the delamanid 6-nitro-2,3-dihydroimidazo[2,1-*b*]oxazole moiety can react easily with a nucleophile. When amino acid residues in HSA attack this carbon, an albumin−delamanid adduct is produced. The delamanid adduct is further hydrolyzed in the presence of water, resulting in the primary metabolite M1. However, further work is necessary to resolve the details of the mechanism.

Albumin, the most abundant protein in plasma (Theodore, 1996), displays pseudo-enzymatic properties, and has been found to catalyze the hydrolysis of numerous compounds, such as cinnamoyl imidazole (Ohta et al., 1983), *p*-nitrophenyl esters (Means and Bender, 1975; Kurono et al., 1979; Watanabe et al., 2000; Sakurai et al., 2004; Lockridge et al., 2008), olmesartan medoxomil (Ma et al., 2005), carbaryl (Sogorb et al., 2004), aspirin (Rainsford et al., 1980; Liyasova et al., 2010), organophosphate insecticides (Sultatos et al., 1984), and long- and short-chain fatty acid esters (Wolfbeis et al., 1987). Among previous studies, the most relevant example of albumin-catalyzed metabolism to this study is that of *N*-trans-cinnamoyl imidazoles (Ohta et al., 1983). It appears that this interaction involves fast acylation of albumin to form cinnamoyl albumin, followed by a slow deacylation of cinnamoyl albumin. The electron-withdrawing substituent, the carbonyl group (C=O) of *N*-trans-cinnamoyl imidazole, facilitates the acylation.

The electron-poor carbon at the C-5 position of the delamanid imidazooxazole structure is also able to react with a nucleophile. Considering the fact that a delamanid analog without the nitro group was not metabolized by HSA (data not shown), an electron-withdrawing nitro group of delamanid is suggested to be important for the propensity toward ring scission by albumin. Ohta et al. (1983) proposed that acylation by albumin occurs at a reactive residue of the R site (Tyr-411), which corresponds to Sudlow's

Site II (Sudlow et al., 1976; Ozeki et al., 1980; Salvi et al., 1997). The nucleophilic character of Tyr-411 for the esterase-like activity toward *p*-nitrophenyl esters was suggested that nucleophilic attack by albumin on the substrate results in an acylated albumin derivative that is then deacylated by general acid or base catalysis (Sakurai et al., 2004). Accordingly, a study using *p*-nitrophenyl acetate as a substrate showed that the enzymatic activity of HSA was dependent on the presence of Tyr-411 (Watanabe et al., 2000). For the protein bindings, at least three binding sites, Site I, Site II, and Site III, are reported to be present on HSA. The saturation of the protein binding capacity of delamanid to HSA (15 μM) was not observed at high concentrations (up to 30 μM; data not shown). Further, the protein binding of delamanid in HSA was not affected by varying the concentrations of Site I–III specific probes (warfarin, diazepam, and digitoxin, respectively; Table 3-4). These results suggest that delamanid may bind non-specifically to HSA. The effects of inhibitory protein binding ligands on delamanid metabolism require further study to clarify the molecular mechanisms of albumin-mediated metabolism.

Esterase-like activity of HSA on olmesartan medoxomil hydrolysis has also been reported (Ma et al., 2005). Chemically modified HSA derivatives (Tyr-, Lys-, His-, and Trp-modifications) and the mutant HSAs K199A, W214A, and Y411A exhibited significantly lower reactivity, suggesting that (wild type) Lys-199, Trp-214, and Tyr-411 play important roles in hydrolysis. Moreover, using selective amino acid reagents, these authors concluded that Cys, Trp, Arg, and Tyr participate in the carbarylase activity of HSA (Sogorb et al., 2004). Finally, it was reported that the bioconversion of aspirin by albumin is a pseudo-esterase reaction in which aspirin stably acetylates lysines on albumin and releases salicylate (Liyasova et al., 2010). These reports collectively suggest that amino acid residues such as lysine, tryptophan and arginine, phenolic hydroxyl groups such as tyrosine, and thiol groups such as cysteine in HSA may be involved in the first step of delamanid metabolism by

albumin.

The overall *in vivo* metabolism of delamanid was qualitatively similar across species, including humans and the predominant preclinical study species. However, quantitative differences were observed among species (Chapter 2). For instance, M1 concentration after repeated administration was much higher in human and dog than in rodents, consistent with the more rapid formation of M1 in human and dog plasma *in vitro* (Fig. 3-2 and Table 3-1). As M1 formation appears to be the primary metabolic reaction of delamanid, it is the determinant of the interspecies differences in delamanid biotransformation.

In conclusion, the new anti-TB drug delamanid is metabolized to (*R*)-2-amino-4,5-dihydrooxazole derivative (M1) by albumin in plasma. The degradation of delamanid by albumin is proposed to begin with attack by amino acid residues of albumin on the electron-poor carbon at the 5 position of nitro-dihydro-imidazooxazole, followed by cleavage of the imidazooxazole moiety to M1.

3.5. Chapter summary

The metabolism of delamanid was investigated *in vitro* using plasma and purified protein preparations from humans and animals. Delamanid was rapidly degraded by incubation in the plasma of all species tested at 37°C, with half-life values (hours) of 0.64 (human), 0.84 (dog), 0.87 (rabbit), 1.90 (mouse), and 3.54 (rat). A major metabolite, M1, was formed in the plasma by cleavage of the 6-nitro-2,3-dihydroimidazo[2,1-*b*]oxazole moiety of delamanid. The rate of M1 formation increased with temperature (0−37°C) and pH (6.0−8.0). Delamanid was not converted to M1 in plasma filtrate, with a molecular mass cutoff of 30 kDa, suggesting that bioconversion is mediated by plasma proteins of higher molecular weight. When delamanid was incubated in plasma protein fractions separated by gel filtration chromatography, M1 was observed in the fraction consisting of albumin, γ-globulin, and α_1-acid glycoprotein. In pure preparations of these proteins, only HSA metabolized delamanid to M1. The formation of M1 followed Michaelis–Menten kinetics in both human plasma and HSA solution with similar K_m values: 67.8 μM in plasma and 51.5 μM in HSA. The maximum velocity and intrinsic clearance values for M1 were also comparable in plasma and HSA. These results strongly suggest that albumin is predominantly responsible for metabolizing delamanid to M1. We propose that delamanid degradation by albumin begins with a nucleophilic attack of amino acid residues on the electron-poor carbon at the 5 position of nitro-dihydro-imidazooxazole, followed by cleavage of the imidazooxazole moiety to form M1.

Chapter 4

In Vitro Inhibitory and Inductive Potential of Delamanid on Cytochrome P450 Enzymes in Human Liver Microsomes and Human Hepatocytes

4.1. Objectives

The inhibitory effects of delamanid have been already investigated on CYP1A2, CYP2A6, CYP2B6, CYP2C8/9, CYP2C19, CYP2D6, CYP2E1, and CYP3A4 activities using human liver microsomes *in vitro*, and delamanid has been reported to have no inhibitory effects on these activities at concentrations up to 100 μM (Matsumoto et al., 2006).

In the present study, we evaluated mechanism-based inactivation (MBI) of delamanid and the inhibitory effects of the metabolites of delamanid on eight CYP enzymes using human liver microsomes *in vitro*. Further, we investigated the inductive effects of delamanid on CYPs including CYP1A2, CYP2B6, CYP2C9, and CYP3A4 in human hepatocytes.

4.2. Materials and Methods

4.2.1. Materials

Delamanid and its metabolites (M1, M2, M3, and M4) were synthesized by Otsuka Pharmaceutical Co., Ltd. 7-Ethoxyresorufin, resorufin, acetaminophen coumarin, bupropion hydrochloride, tolbutamide, hydroxytolbutamide, paclitaxel, diclofenac sodium salt, (±)-bufuralol hydrochloride salt, (±)-hydoxybufuralol maleate salt, chlorzoxazone, nifedipine, testosterone, and 6β-hydroxytestosterone were purchased from Sigma-Aldrich Co. Other chemicals were obtained from the following sources: phenacetin, 7-hydroxycoumarin, and midazolam from Wako Pure Chemical Industries, Ltd.; hydroxybupropion, 6α-hydroxypaclitaxel, and 4-hydroxydiclofenac from Becton, Dickinson and Company; *S*-(+)-mephenytoin, (±)-4-hydroxymephenytoin, 6-hydroxychlorzoxazone and

1-hydroxymidazolam from Toronto Research Chemicals, Inc.; oxidized nifedipine from Oxford Biomedical Research. All reagents and solvents were of analytical grade or higher. Human liver microsomes were supplied by Becton, Dickinson and Company (50 donors and 150 donors) and Xenotech, LLC (50 donors). Human fresh individual hepatocytes prepared by Xenotech, LLC were used. Cryopreserved human individual hepatocytes were purchased from Celsis IVT.

4.2.2. Inhibitory Effects on Cytochrome P450s

The inhibitory potential of metabolites (M1, M2, M3, and M4) was evaluated and determined with the modified methods in previous reports (Ikeda et al., 2001; Matsumoto et al., 2006). The experimental conditions used in the inhibitory study are described in Tables 4-1 and 4-2. Substrates were dissolved in appropriate solvents. The final concentration of these solvents in each reaction mixture was less than 1% (v/v). Metabolites (test products) and known CYP inhibitors (positive controls) were freshly prepared in DMSO, and the DMSO concentration was 0.5% (v/v) in incubation mixtures. Human liver microsomes supplied by Xenotech, LLC were used for metabolites, M1 and M4, and those supplied by Becton, Dickinson and Company (150 donors) were used for metabolites, M2 and M3. Incubation mixtures were prepared on ice, without NADPH generating system (or NADPH/NADH) or without substrate, in the test product (1, 3, 10, 30, or 100 μM), positive control or vehicle control with pH 7.4 phosphate buffer (100 mM) using human liver microsomes (0.02–1 mg/mL). Incubation mixtures were then pre-incubated at 37°C. Each reaction was initiated by the addition of the NADPH-generating system (or NADPH/NADH) or the substrate solution, and the mixtures were then incubated at 37°C. Each reaction was terminated with an appropriate stop reagent. Reactions were conducted in duplicate.

Table 4-1 Experimental conditions used in inhibitory study for delamanid's metabolites, M1 and M4.

CYP Isoforom	Substrate	Solvent	(μM)	Protein (mg/mL)	Incubation Time (min)	Stop Solution	Positive Control	(μM)	Remaining Activity (%)
CYP1A2	7-Ethoxyresorufin	a	0.5	0.2	10	a	α-Naphthoflavone	0.1	6.0
CYP2A6	Coumarin	b	1	0.2	2	a	8-Methoxypsoralen	0.2	7.5
CYP2B6	Bupropion	b	100	0.2	30	a	Ticlopidine	0.2	15.0
CYP2C8/9	Tolbutamide	b	250	0.2	30	a	Sulfaphenazole	50	11.2
CYP2C19	*S*-Mephenytoin	b	20	0.2	30	a	Tranylcypromine	25	15.8
CYP2D6	Bufuralol	b	10	0.2	20	a	Quinidine	1	17.9
CYP2E1	Chlorzoxazone	b	40	0.2	30	a	Diethyldithiocarbamate	200	20.3
CYP3A4	Nifedipine	a	30	0.2	10	a	Ketoconazole	0.5	8.9
CYP3A4	Testosterone	b	50	0.2	10	a	Ketoconazole	0.5	4.3

a: Acetonitrile; b: Methanol. Vehicle control activity was 18.9, 465.0, 148.0, 81.8, 13.0, 38.5, 97.3, 1730.0, and 1430.0 pmol/min/mg for CYP1A2, CYP2A6, CYP2B6, CYP2C8/9, CYP2C19, CYP2D6, CYP2E1, CYP3A4 (nifedipine), and CYP3A4 (testosterone), respectively. Each activity represents the mean of the data in duplicate.

Table 4-2 Experimental conditions used in inhibitory study for delamanid's metabolites, M2 and M3.

CYP Isoforom	Substrate	Solvent	(μM)	Protein (mg/mL)	Incubation Time (min)	Stop Solution	Positive Control	(μM)	Remaining Activity (%)
CYP1A2	7-Ethoxyresorufin	a	0.5	0.4	10	b	α-Naphthoflavone	0.1	11.0
CYP2A6	Coumarin	b	2	0.05	30	e	8-Methoxypsoralen	1	11.7
CYP2B6	Bupropion	c	100	0.2	30	e	Ticlopidine	0.2	48.6
CYP2C8/9	Tolbutamide	c	400	0.5	60	f	Sulfaphenazole	100	16.1
CYP2C19	*S*-Mephenytoin	c	100	0.5	60	e	Tranylcypromine	100	11.1
CYP2D6	Bufuralol	b	20	1	30	e	Quinidine	100	5.7
CYP2E1	Chlorzoxazone	d	100	0.5	15	g	Diethyldithiocarbamate	300	42.9
CYP3A4	Nifedipine	b	50	0.5	10	g	Ketoconazole	100	0.0
CYP3A4	Testosterone	c	100	0.02	10	e	Ketoconazole	100	0.0

a: Acetonitrile; b: Ethanol; c: Methanol; d: 1% (w/v) Sodium carbonate aqueous solution; e: Chlorpropamide/Acetonitrile; f: Hydrochloric acid; g: Ethyl acetate. Vehicle control activity was 11.7, 270.5, 107.2, 67.3, 19.6, 24.1, 392.4, 1961.2, and 3838.0 pmol/min/mg for CYP1A2, CYP2A6, CYP2B6, CYP2C8/9, CYP2C19, CYP2D6, CYP2E1, CYP3A4 (nifedipine), and CYP3A4 (testosterone), respectively. Each activity represents the mean of the data in duplicate.

Calibration curves were constructed to accurately quantitate the activity of each CYP enzyme under evaluation (CYP1A2, CYP2A6, CYP2B6, CYP2C8/9, CYP2C19, CYP2D6, CYP2E1, and CYP3A4). Analysis of inhibition of enzymatic activity for each test product, positive control or vehicle control was conducted by HPLC or LC-MS/MS. No marked difference was observed between vehicle control activities, even though the studies were performed under different conditions (Tables 4-1, 4-2). The inhibitory activity of each concentration of each test product or positive control was calculated as the percent difference of remaining activity with respect to the vehicle control. The IC_{50} values for each test product were obtained using WinNonlin (Pharsight). The I/K_i values, where I is inhibitor concentration from the C_{max} following twice daily administration of 100 mg delamanid in humans and K_i is $0.5 \times IC_{50}$ [as the substrate concentration is investigated by approximately K_m (Tables 4-1, 4-2)], were calculated for test products with IC_{50} values <100 μM.

The potential for MBI of delamanid in each CYP isoform was further investigated. Human liver microsomes [Becton, Dickinson and Company (50 donors), 0.2–5 mg/mL] were incubated at 37°C for 30 min in pH 7.4 phosphate buffer (100 mM) for five conditions (first incubation), #1 (enzyme), #2 {enzyme+test product [delamanid (100 μM)]}, #3 [enzyme+NADPH (2.5 mM)], #4 {enzyme+test product [delamanid (100 μM)]+NADPH (2.5 mM)}, and #5 [enzyme+positive control+NADPH (2.5 mM)]. Following the first incubation, an aliquot of each mixture was added to a second mixture containing NADPH/NADH in pH 7.4 phosphate buffer (100 mM). The experimental conditions used in the inhibitory study for the second incubation are described in Table 4-3.

Table 4-3 Experimental conditions used in MBI study for delamanid.

CYP Isoforom	Substrate (μM)		Protein (mg/mL)	Incubation Time (min)	Positive Control (μM)	
CYP1A2	Phenacetin	50	0.2	20	Furafylline	10 [a]
CYP2A6	Coumarin	5	0.1	10	8-Methoxypsoralen	10 [a]
CYP2B6	Bupropion	50	0.2	10	Ticlopidine	10 [a]
CYP2C8	Paclitaxel	10	0.2	20	Quercetin	50
CYP2C9	Diclofenac	5	0.05	20	Sulfaphenazole	10
CYP2C19	*S*-Mephenytoin	100	0.5	30	Tranylcypromine	50
CYP2D6	Bufuralol	20	0.2	20	Quinidine	10
CYP3A4	Testosterone	100	0.02	10	Ketoconazole	10
CYP3A4	Midazolam	5	0.05	20	Ketoconazole	10

[a] Each value represents the concentration of the first incubation. Reaction mixture for the second incubation contained pH 7.4 phosphate buffer (100 mM), NADPH/NADH (2.5 mM), first incubation mixture diluted by 10-fold, and each substrate.

Substrates and positive controls were dissolved in DMSO. CYP substrates were then added and these reaction mixtures were incubated at 37°C until termination with chlorpropamide/acetonitrile. Incubations were performed in duplicate. Calibration curves were constructed to accurately quantitate the activity of each CYP enzyme under evaluation. Following the second incubation, analysis of each enzymatic activity for conditions #1 to #5 was conducted by LC-MS/MS. The activity of each enzymatic reaction (condition #2 or #4 and #5) was compared with that of the corresponding control (condition #1 or #3) and expressed as a percentage of that control. The difference of the remaining activity was then calculated between samples with and without NADPH. It is reported that a decrease in activity of 15.0% is identified as the cutoff value for identifying inactivators for CYP enzymes (Obach et al., 2007). It was prospectively determined that % difference of remaining activity, <15.0% would have little potential for MBI for the corresponding isoform.

4.2.3. Inductive Effects on Cytochrome P450s

Hepatocytes were isolated and cultured according to previously described methods (Quistorff et al., 1990; LeCluyse et al., 1994; LeCluyse et al., 1996; Robertson et al., 2000; Mudra et al., 2001; Madan et al., 2003). Three lots of human fresh hepatocytes were used for the assessment of CYP1A2, CYP2C9, and CYP3A4 activities and the relative mRNA levels. Hepatocytes were seeded at approximately 1.3×10^6 viable cells/mL on collagencoated 60 mm culture dishes and were placed in a humidified culture chamber (37°C, at 95% relative humidity, 95/5% air/carbon dioxide). After two to three hours, the media was replaced with modified Chee's medium (MCM) containing ITS+ (6.13 μg/mL insulin, 6.13 μg/mL transferrin and 6.13 ng/mL selenous acid), linoleic acid (5.25 μg/mL), bovine serum albumin (1.23 mg/mL), penicillin (49 U/mL), streptomycin (49 μg/mL), dexamethasone (0.098 μM),

and Matrigel (250 μg/mL). Cultures were allowed to adapt to the culture environment for three days, with daily replacement of supplemented MCM (without Matrigel). After the adaptation period, hepatocyte cultures were then treated daily for three consecutive days with supplemented MCM containing 0.1% (v/v) DMSO (vehicle control), one of three concentrations of delamanid (0.1, 1, or 10 μM), 100 μM omeprazole [CYP1A2 inducer (positive control)], or 10 μM rifampin [CYP2C9 and CYP3A4 inducer (positive controls)]. Following the exposure period, microsomal samples were prepared from the human hepatocytes based on the method described previously (Madan et al., 1999) and were stored at −80°C.

Microsomal incubations were conducted at 37°C in incubation mixtures containing potassium phosphate buffer (50 mM, pH 7.4), $MgCl_2$ (3 mM), ethylenediaminetetraacetic acid (1 mM), nicotinamide adenine dinucleotide phosphate (NADP) (1 mM), glucose-6-phosphate (5 mM), glucose-6-phosphate dehydrogenase (1 Unit/mL), and a substrate. The substrates were phenacetin (80 μM) for CYP1A2, diclofenac (100 μM) for CYP2C9, and testosterone (250 μM) for CYP3A4. Reactions were started by the addition of the NADPH-generating system and were stopped after 30 min (for CYP1A2) or 10 min (for CYP2C9 and CYP3A4) by the addition of acetonitrile containing the internal standard (d4-acetaminophen for CYP1A2, d4-4-hydroxydiclofenac for CYP2C9, or d3-6β-hydroxytestosterone for CYP3A4. Precipitated protein was removed by centrifugation and supernatant fractions were analyzed by LC-MS/MS to determine CYP enzyme activities.

Approximately 24 h after the last treatment, total RNA was extracted using the TRIzol (Invitrogen) and purified using the RNeasy Mini Kit (Qiagen). The RNA integrity was analyzed with the RNA 6000 Nano Assay Kit (Agilent Technologies). Single-stranded cDNA was prepared from total mRNA using High Capacity cDNA Reverse Transcription Kit (Applied Biosystems). The amplification was carried out in a total volume of 20 μL using

TaqMan Gene Expression Master Mix (Applied Biosystems) with an Applied Biosystems 7300 Real Time polymerase chain reaction (PCR) sequence detection system. CYP1A2, CYP2C9, CYP3A4, and glyceraldehyde-3-phosphate dehydrogenase (GAPDH) mRNA expression levels were measured with real-time reverse transcription (RT)-PCR using TaqMan gene expression assays (Applied Biosystems), including CYP1A2 (assay ID: Hs00167927_m1), CYP2C9 (assay ID: Hs00426397_m1), CYP3A4 (assay ID: Hs00604506_m1), and GAPDH (assay ID: Hs99999905_m1) primer sets. The relative mRNA levels of target genes were determined by normalizing the raw data to the GAPDH mRNA level. The relative gene expression was determined by the comparative *C*t method (ΔΔCT method).

Three lots of cryopreserved human hepatocytes were used for the effects of delamanid on CYP2B6 mRNA levels. Hepatocytes were thawed in *InVitro*GRO CP Medium (Celsis IVT) supplemented with Torpedo Antibiotic Mix (Celsis IVT) and seeded at 0.7×10^6 viable cells/mL in collagen-coated 24-well plates. After 4 h, media was changed to the supplemented CP Medium, and hepatocytes were cultured for 2 d with daily replacement with the supplemented CP Medium. Following a 2-d adaptation period, hepatocytes were then treated daily for two consecutive days with *InVitro*GRO HI Medium containing 0.1% (v/v) DMSO (vehicle control), one of three concentrations of delamanid (0.1, 1, or 10 μM), or 750 μM phenobarbital [CYP2B6 inducer (positive control)].

Approximately 24 h after the last treatment, total RNA was extracted from the additional culture of hepatocytes and purified using RNeasy Micro Kit (Qiagen). The RNA integrity was analyzed by the same method as described above. Single-stranded cDNA was prepared from total mRNA using Transcriptor First Strand cDNA Synthesis Kit (Roche Diagnostics, Mannheim, Germany). The amplification was carried out using LightCycler 480 Probes Master (Roche Diagnostics) with LightCycler 480 II sequence detection system

(Roche diagnostic). CYP2B6 and hypoxanthine phosphoribosyltransferase 1 (HPRT1) mRNA expression levels were measured with real-time RT-PCR using TaqMan gene expression assays (Applied Biosystems), including CYP2B6 (assay ID: Hs04183483_g1) and HPRT1 (assay ID: Hs02800695_m1) primer sets. The mRNA levels were determined by normalizing the raw data to the HPRT1 mRNA level. The relative gene expression was according to the same method as other CYP isoforms.

4.2.4. Data Processing

All inhibition data were calculated using the mean of the data in duplicate. All induction data about CYP enzyme activities and mRNA levels were shown as the mean±S.D. of the data from three individual hepatocyte preparations. Fold increase was expressed as the ratio of the CYP enzyme activities and mRNA levels of compoundtreated groups to that of vehicle-treated group. Percent positive control was calculated as follows. Percent positive control (%)={[(fold change in treated sample)−1]/[(fold change in positive control)−1]}×100

4.3. Results

4.3.1. Inhibitory Effects on Cytochrome P450s

The inhibitory potential of delamanid's metabolites (M1, M2, M3, and M4) (1–100 μM) on the catalytic activities of eight CYP isoforms in human liver microsomes is presented in Table 4-4. The positive control inhibitors used in each experiment produced the expected inhibitory effects on the activities of the corresponding CYP isoforms (Tables 4-1, 4-2). Metabolites at concentrations up to 100 μM inhibited the activities of multiple CYP isoforms,

though to varying extents. M1 inhibited the activities of all CYP isoforms except for CYP2E1-mediated activity with the IC_{50} values between 18.3 and 87.5 μM. M2 inhibited CYP2A6 and CYP2B6 activities with the IC_{50} values of 42.3 and 32.7 μM, respectively. This metabolite also inhibited CYP3A4 activity with the IC_{50} value of 10.9 μM when testosterone 6β-hydroxylation was used as the metabolic test reaction, but was much less effective at inhibiting the CYP3A4 activity when nifedipine oxidation was examined (IC_{50}>100 μM). M3 slightly inhibited CYP2B6, CYP2C8/9, and CYP2C19 activities, but no IC_{50} values fell below 100 μM (IC_{50}>100 μM). M4 inhibited CYP2B6, CYP2C8/9, and CYP2C19 activities with the IC_{50} values between 25.2 and 89.4 μM.

Our previous paper indicates that delamanid does not inhibit any activities of the CYP isoforms (IC_{50}>100 μM) (Matsumoto et al., 2006). The I/K_i values for delamanid and each of its metabolites that had IC_{50} values less than 100 μM are presented in Table 4-5. The C_{max} (I value) for delamanid based on twice daily oral administration of 100 mg delamanid for 2 months (56 d) in combination with a background drug regimen in humans has been reported to be 0.78 μM (Gler et al., 2012). Maximal concentrations for its metabolites were determined to be 0.32 μM for M1, 0.12 μM for M2, 0.22 μM for M3, and 0.13 μM for M4 (Chapter 2). The IC_{50} values of metabolites from the *in vitro* study were at least 50 times higher than the plasma concentrations of metabolites in humans. The I/K_i values calculated for the metabolites M1, M2, and M4 were between 0.003 and 0.035.

The potential for MBI of delamanid in each CYP isoform was investigated using human liver microsomes. These results are shown in Table 4-6. The positive control inhibitors used in each experiment produced the expected inhibitory effects on the CYP activities. The difference of the remaining activity between samples with and without NADPH (condition #2 and #4, respectively) for delamanid (100 μM) during the first incubation was less than 13.8%. Delamanid was considered to have little potential for MBI.

Table 4-4 IC_{50} values of delamanid and its metabolites for CYP enzymes in human liver microsomes.

CYP Isoform	Metabolic Reaction	IC_{50} (μM)				
		Delamanid [a]	M1	M2	M3	M4
CYP1A2	7-Ethoxyresorufin *O*-deethylation	> 100	41.0	> 100	> 100	> 100
CYP2A6	Coumarin 7-hydroxylation	> 100	87.5	42.3	> 100	> 100
CYP2B6	Bupropion hydroxylation	> 100	24.3	32.7	> 100	25.2
CYP2C8/9	Tolbutamide methylhydroxylation	> 100	30.7	> 100	> 100	42.9
CYP2C19	*S*-Mephenytoin 4'-hydroxylation	> 100	18.3	> 100	> 100	89.4
CYP2D6	Bufuralol 1'-hydroxylation	> 100	28.9	> 100	> 100	> 100
CYP2E1	Chlorzoxazone 6-hydroxylation	> 100	> 100	> 100	> 100	> 100
CYP3A4	Nifedipine oxidation	> 100	53.6	> 100	> 100	> 100
CYP3A4	Testosterone 6β-hydroxylation	> 100	35.8	10.9	> 100	> 100

[a] IC_{50} values of delamanid were calculated from previous report (Matsumoto et al., 2006). Each value was calculated using the mean of the data in duplicate for each metabolite. IC_{50} values were calculated when the mean remaining activity at 100 μM was less than 50% of control.

Table 4-5 Assessment of DDI risk of delamanid and its metabolites.

CYP Isoform	I/K_i				
	Delamanid	M1	M2	M3	M4
CYP1A2	ND	0.016	ND	ND	ND
CYP2A6	ND	0.007	0.006	ND	ND
CYP2B6	ND	0.026	0.007	ND	0.010
CYP2C8/9	ND	0.021	ND	ND	0.006
CYP2C19	ND	0.035	ND	ND	0.003
CYP2D6	ND	0.022	ND	ND	ND
CYP2E1	ND	ND	ND	ND	ND
CYP3A4	ND	0.012	ND	ND	ND
CYP3A4	ND	0.018	0.022	ND	ND

***I* = inhibitor concentration from the maximal circulating plasma concentration; K_i = inhibition constant.**

ND = not determined, as IC_{50} was above 100 μM. K_m = Michaelis constant.

K_i was calculated by the following equation, $K_i = 0.5 \times IC_{50}$, as the substrate concentration was investigated by approximately K_m.

Table 4-6 Potential for MBI of delamanid on CYP enzymes in human liver microsomes.

CYP Isoform	Metabolic Reaction	Remaining Activity (%)		% Difference of Remaining Activity	Potential of MBI	Remaining Activity (%)
		Condition #2	Condition #4			Condition #5
CYP1A2	Phenacetin *O*-deethylation	97.5	111.3	13.8	Little potential	4.9
CYP2A6	Coumarin 7-hydroxylation	97.1	92.6	4.5	Little potential	2.5
CYP2B6	Bupropion hydroxylation	92.5	94.3	1.8	Little potential	2.7
CYP2C8	Paclitaxel 6α-hydroxylation	102.7	106.1	3.4	Little potential	5.2
CYP2C9	Diclofenac 4'-hydroxylation	95.9	87.7	8.2	Little potential	2.7
CYP2C19	*S*-Mephenytoin 4'-hydroxylation	109.1	96.0	13.1	Little potential	10.1
CYP2D6	Bufuralol 1'-hydroxylation	96.9	96.1	0.8	Little potential	8.6
CYP3A4	Testosterone 6β-hydroxylation	92.4	88.2	4.2	Little potential	28.9
CYP3A4	Midazolam 1'-hydroxylation	106.6	95.6	11.0	Little potential	0.1

Each value was calculated using the mean of the data in duplicate. Remaining activity of condition #2 (enzyme + test product) or #4 (enzyme + test product + NADPH) and #5 (enzyme + positive control + NADPH) was compared with that of the corresponding control [condition #1 (enzyme) or #3 (enzyme + NADPH)] and expressed as a percentage of control. Percent (%) difference of remaining activity, < 15.0% would have little potential for mechanism-based inactivation for the corresponding isoform.

4.3.2. Inductive Effects on Cytochrome P450s

The effects of delamanid on the enzymatic activities of CYP1A2, CYP2C9, and CYP3A4 and on mRNA levels for these enzymes were examined using freshly isolated human hepatocytes. In addition, its effects on CYP2B6 were investigated at mRNA levels using cryopreserved human hepatocytes. These results are shown in Tables 4-7 and 4-8. The human hepatocytes from three different donors were independently used, and the results were expressed as the mean±S.D. of the data from three individual hepatocyte preparations. Treatment of cultured hepatocytes with the positive controls omeprazole (CYP1A2), phenobarbital (CYP2B6), or rifampin (CYP2C9 and CYP3A4) caused the anticipated increases in isoform-specific activities and corresponding mRNA levels. Hepatocyte cultures that were similarly treated with delamanid at concentrations up to 10 μM showed no changes in CYP1A2 and CYP2C9 activities and relative mRNA levels. No effects on CYP2B6 mRNA levels were observed at 0.1 and 1 μM delamanid concentrations, and only a marginal increase of 1.48-fold was observed in hepatocyte culture treated with delamanid at 10 μM. Three days of treatment with delamanid at concentrations up to 1 μM had no effects on CYP3A4 activities and CYP3A4 mRNA levels. Treatment with delamanid at a concentration of 10 μM had a minimal overall effect on CYP3A4 mRNA levels with an increase of 1.49-fold relative to the vehicle control (DMSO) (Table 4-8). However, identically treated hepatocyte cultures showed an overall decrease in CYP3A4 activities to 0.672-fold, compared with the vehicle control (Table 4-7).

Table 4-7 Effects of delamanid on microsomal CYP enzyme activities in human hepatocytes.

Treatment	Concentration (μM)	Enzyme Activities (Fold Increase)		
		Phenacetin *O*-dealkylation	Diclofenac 4´-hydroxylation	Testosterone 6β-hydroxylation
		CYP1A2	CYP2C9	CYP3A4
DMSO (Vehicle)	0.1% (v/v)	1.00 ± 0.62	1.00 ± 0.47	1.00 ± 0.52
Delamanid	0.1	1.01 ± 0.19	1.04 ± 0.12	1.17 ± 0.22
Delamanid	1	1.01 ± 0.05	1.08 ± 0.02	0.945 ± 0.153
Delamanid	10	1.05 ± 0.21	1.05 ± 0.07	0.672 ± 0.217
Omeprazole	100	15.0 ± 6.5	1.69 ± 0.31	2.16 ± 0.64
Rifampin	10	1.66 ± 0.83	2.42 ± 0.33	5.86 ± 2.51

Vehicle control activities in 0.1% (v/v) DMSO were 61.1 ± 38.1, 1120 ± 520, and 2570 ± 1340 pmol/min/mg for CYP1A2, CYP2C9, and CYP3A4 catalyzed reactions, respectively. Each value represents the mean ± SD of the data from three individual hepatocyte preparations.

Table 4-8 Effects of delamanid on CYP mRNA levels in human hepatocytes.

Treatment	Concentration (μM)	CYP mRNA Levels (Fold Increase)			
		CYP1A2	CYP2B6	CYP2C9	CYP3A4
DMSO (Vehicle)	0.1% (v/v)	1.00 ± 0.00	1.00 ± 0.00	1.00 ± 0.00	1.00 ± 0.00
Delamanid	0.1	0.908 ± 0.146	1.12 ± 0.04	0.911 ± 0.105	1.09 ± 0.21
Delamanid	1	1.07 ± 0.22	1.24 ± 0.18	0.892 ± 0.061	0.953 ± 0.234
Delamanid	10	1.22 ± 0.61	1.48 ± 0.19	1.04 ± 0.24	1.49 ± 0.61
Omeprazole	100	277 ± 208	NT	1.74 ± 0.73	2.78 ± 1.09
Phenobarbital	750	NT	10.4 ± 2.1	NT	NT
Rifampin	10	1.85 ± 1.53	NT	3.28 ± 1.09	9.84 ± 5.96

NT = Not tested. Each value represents the mean ± SD of the data from three individual hepatocyte preparations.

Experiments were conducted using freshly isolated human hepatocytes for CYP1A2, CYP2C9, and CYP3A4 and cryopreserved human hepatocytes for CYP2B6.

4.4. Discussion

Examination of delamanid's effects on CYP inhibition and induction is an important first step in the planning of clinical trials examining delamanid's interactions with other concomitantly administered medications. We have already reported that delamanid had no competitive inhibition on the activities of eight CYP isoforms in a previous study (Matsumoto et al., 2006). In the present study, we investigated first MBI by delamanid on CYP enzymes. The results of the *in vitro* experiments indicated that delamanid (100 μM) appeared to have little potential for MBI (Table 4-6).

Following oral administration of delamanid to humans and animals, at least four metabolites, M1, M2, M3, and M4, have been detected and identified in the plasma (Chapter 2). Further, the C_{max} for delamanid has been reported to be 0.78 μM following twice daily administration of 100 mg delamanid for 56 d in clinical trial (Gler et al., 2012). The C_{max} values for its metabolites were determined to be 0.32 μM for M1, 0.12 μM for M2, 0.22 μM for M3, and 0.13 μM for M4, suggesting that M1 is the most abundant metabolite in humans (Chapter 2). The inhibitory effects of delamanid and its metabolites are considered to be minimal based on these plasma concentrations in humans. However, it is more important to evaluate this based on hepatic concentrations where CYP enzymes exist. In an *in vivo* study, the concentrations of delamanid and metabolites in liver were investigated in rats following repeated oral administration of delamanid. The results indicated that delamanid was observed in the liver at a high concentration of approximately 6 times that of the maximal plasma concentration (not reported). If the liver/plasma concentration ratio in humans is the same as that in rats, delamanid is presumed to be also no inhibitory effects on CYP enzymes based on human hepatic concentrations.

With the background of the metabolism of delamanid, we investigated additionally the inhibition potential of four metabolites. The inhibitory effects of delamanid's metabolites were observed only at metabolite concentrations exceeding those observed in human plasma during clinical trials. While the metabolites M2, M3, and M4 in rat liver were not detected, the metabolite M1 was observed at a concentration of approximately 30% of delamanid (not reported). If the distribution of M1 in liver is the same as that of delamanid, the maximal liver concentration for M1 in humans is presumed to be approximately 2 μM. The *I*/*K*i values from liver concentration are calculated to be <0.22. Considering that the plasma protein binding of M1 is extremely high, approximately 99.7% (0.3% as free form, Chapter 2), free concentration of M1 around an enzyme site in the liver is presumed to be lower, suggesting that M1 has a low potential to induce DDIs due to the inhibition of CYP enzymes. The potential for MBI of delamanid's metabolites was not investigated in the present study. Additional work may be necessary to study MBI of the principal metabolites in the future.

In the inhibitory study, one metabolite, M2, inhibited testosterone 6β-hydroxylase (IC_{50} of 10.9 μM), but not nifedipine oxidase (IC_{50}>100 μM). Nifedipine has been reported to have freedom of movement and can bind to multiple CYP3A4 active sites, including the testosterone binding site, whereas testosterone is fixed to a certain part of the active site (Wang et al., 2000). The inhibition results suggest that M2 inhibits only a certain part of the active site for testosterone, not multiple sites.

According to the European Medicines Agency guideline (http://www.ema.europa.eu/docs/en_GB/document_library/Scientific_guideline/2012/07/WC500129606.pdf), the *in vitro* study should be considered as a positive for the enzyme induction when the incubations with the test drug give rise to a more than a 2-fold increase in mRNA and the increases are seen in a concentration-dependent manner. In addition, an observed concentration-dependent increase in mRNA of <100% can be considered as a negative only when the increase in

mRNA is less than 20% of the response of the positive control (percent positive control). In the present study, the extent of the increase in mRNA levels of CYP1A2, CYP2B6, CYP2C9, and CYP3A4 was less than 1.49-fold in all delamanid-treated groups (Table 4-8). The maximal value of percent positive control was 6% in CYP3A4 mRNA levels for 10 μM delamanid. In the same manner, the enzymatic activities of CYP1A2, CYP2C9, and CYP3A4 for delamanid were less than 1.17-fold increase of control (Table 4-7). Consequently, the delamanid ($\leq$10 μM) showed no inductive effects on the enzymatic activities and mRNA levels of four CYP enzymes in cultured human hepatocytes.

Treatment with up to 1 μM delamanid had also no effect on CYP3A4 activities and CYP3A4 mRNA levels. However, treatment with 10 μM delamanid resulted in an anomalous result, *i.e.*, a small decrease in CYP3A4 activities and a slight increase (1.49-fold) in CYP3A4 mRNA levels. The reason for this discordant result is unclear. It may be possible that one or more metabolite(s) having CYP3A4 inhibitory activity was produced during culturing human hepatocytes with delamanid. Further work will be necessary to resolve this apparent discordant result.

In conclusion, delamanid ($\leq$100 μM) showed no inhibitory effects on eight CYP isoforms and had little potential for MBI. Delamanid's metabolites were noted to inhibit some CYP isoforms, but these effects were observed only at metabolite concentrations that were well above those observed in human plasma. Delamanid ($\leq$10 μM) did not induce CYP1A2, CYP2B6, CYP2C9, and CYP3A4 in human hepatocytes. These data suggest that delamanid is unlikely to cause clinically relevant CYP-mediated drug interactions.

4.5. Chapter summary

The ability of delamanid to inhibit or induce CYP enzymes was investigated *in vitro* using human liver microsomes or human hepatocytes. Delamanid (100 μM) had little potential for MBI on eight CYP isoforms (CYP1A2, CYP2A6, CYP2B6, CYP2C8, CYP2C9, CYP2C19, CYP2D6, and CYP3A4). Delamanid's metabolites were noted to inhibit the metabolism of some CYP isoforms, but these effects were observed only at metabolite concentrations that were well above those observed in human plasma during clinical trials. Delamanid ($\leq$10 μM) did not induce CYP1A2, CYP2C9, and CYP3A4 activities in human hepatocytes, and there were no increases in CYP1A2, CYP2B6, CYP2C9, and CYP3A4 mRNA levels. Taken together, these data suggest that delamanid is unlikely to cause clinically relevant DDIs when co-administered with products that are metabolized by the CYP enzyme system.

Chapter 5

In Vitro Inhibitory Potential of Twenty Five Anti-Tuberculosis Drugs on Cytochrome P450 Activities in Human Liver Microsomes

5.1. Objectives

Information on the CYP inhibitory potential for anti-TB drugs both *in vivo* and *in vitro* is limited. It is therefore critical to understand the ability of anti-TB drugs to inhibit CYP enzymes. In the present study, twenty five anti-TB drugs were selected by reference to a WHO guideline published in 2011 (http://whqlibdoc.who.int/publications/2011/9789241-501583_eng.pdf). To predict DDIs, the direct inhibitory effects of these anti-TB drugs on eight substrate reactions for seven CYP enzymes were evaluated using human liver microsomes *in vitro*.

5.2. Materials and Methods

5.2.1. Materials

Isoniazid, rifampicin, ethambutol dihydrochloride, pyrazinamide, rifabutin, levofloxacin, ofloxacin, ethionamide, D-cycloserine, *p*-aminosalicylic acid, clofazimine, linezolid, potassium clavulanate, clarithromycin, and imipenem monohydrate were purchased from Sigma-Aldrich. Rifapentine, moxifloxacin hydrochloride, capreomycin sulfate, and thioacetazone were purchased from Santa Cruz Biotechnology. Streptomycin sulfate, kanamycin A, amikacin disulfate, gatifloxacin, and prothionamide were purchased from LKT Laboratories. Amoxicillin trihydrate was purchased from Tokyo Chemical Industry. CYP enzyme-specific marker substrates, metabolites, positive controls, and internal standards were purchased from Wako Pure Chemical Industries, Sigma-Aldrich, Toronto Research Chemicals, Corning, Tokyo Chemical Industry, Santa Cruz Biotechnology, and Alsachim. NADPH and NADH were purchased from Oriental Yeast. Pooled human liver microsomes

(150 donors) were supplied by Corning. All other chemicals and solvents were of the highest chemical grade available.

5.2.2. Incubation Conditions

The standard incubation mixture consisted of 100 mM potassium phosphate buffer (pH 7.4), 2.5 mM NADPH/NADH mixture solution, microsomes, a substrate, and a test compound or a positive control inhibitor. The experimental conditions for CYP inhibitory assays are summarized in Table 5-1. Substrate was incubated at a concentration equal to previously determined Michaelis–Menten constant (K_m) value. The substrates and inhibitors were dissolved in acetonitrile/DMSO (9:1, v/v) or methanol (bupropion). The test compounds at seven concentrations were prepared in DMSO, acetonitrile/DMSO (9:1, v/v), or saline. The final concentration of organic solvents in each reaction mixture was 1% (v/v) or less. The highest concentration of test compounds was set at equal to or more than the C_{max} in human plasma. After preincubation at 37°C for 5 min, the reaction was initiated by adding NADPH/NADH solution in a final volume of 400 μL in duplicate. After the incubation, the reaction was terminated with 400 μL of ice-cold acetonitrile/methanol (1:1, v/v) containing each internal standard. Those samples and standard curve samples were centrifuged at 5013 ×*g* for 10 min, and the supernatants were subjected to HPLC separation with LC–MS/MS.

Table 5-1 Summary of experimental conditions for CYP inhibitory assays.

CYP enzyme	Reaction	Substrate	(μM)	Incubation time (min)	Protein (mg/mL)	Positive control	(μM)
CYP1A2	Phenacetin *O*-deethylation	Phenacetin	50	20	0.1	α-Naphthoflavone	1
CYP2B6	Bupropion hydroxylation	Bupropion	150	20	0.1	Sertraline	50
CYP2C8	Paclitaxel 6α-hydroxylation	Paclitaxel	10	20	0.1	Quercetin	50
CYP2C9	Diclofenac 4′-hydroxylation	Diclofenac	10	10	0.1	Sulfaphenazole	10
CYP2C19	S-Mephenytoin 4′-hydroxylation	*S*-Mephenytoin	30	30	0.2	Tranylcypromine	50
CYP2D6	Bufuralol 1′-hydroxylation	Bufuralol	10	10	0.1	Quinidine	10
CYP3A4 (M[a])	Midazolam 1′-hydroxylation	Midazolam	2	10	0.1	Ketoconazole	10
CYP3A4 (T[b])	Testosterone 6β-hydroxylation	Testosterone	100	10	0.1	Ketoconazole	10

[a]Midazolam; [b]Testosterone

5.2.3. Liquid Chromatography-Tandem Mass Spectrometry Analysis

All measurements were conducted using an API4000 or 4000QTRAP mass spectrometer (AB Sciex) and a Prominence HPLC system (Shimadzu). The measurement by LC–MS/MS was operated in the multiple reaction monitoring (MRM) mode and the positive mode for electrospray ionization. The metabolite used in the analytical method was acetaminophen for CYP1A2; hydroxybupropion for CYP2B6; 6α-hydroxypaclitaxel for CYP2C8; 4′-hydroxydiclofenac for CYP2C9; 4′-hydroxymephenytoin for CYP2C19; 1′-hydroxybufuralol for CYP2D6; 1′-hydroxymidazolam for CYP3A4 (M), and 6β-hydroxytestosterone for CYP3A4 (T). Each stable isotope was used as the internal standard. HPLC separation was performed using a Cadenza CD-C18 (2.0 × 100 mm, 3 μm; Imtakt) and with mobile phase A [1 mM ammonium formate aqueous/formic acid (1000:2, v/v)] and B (methanol). The gradient program was 10 (0.0–1.0) → 90 (5.0–9.0) → 10 (9.1–15.0) (%B (min)), and the flow rate was 0.25 mL/min. For all measurements, the column oven temperature was set at 40°C.

5.2.4. Data Analysis

All inhibition data were calculated using the mean of data in duplicate. The IC_{50} values were calculated using Phoenix WinNonlin version 6.3 (Pharsight). The inhibition constant (K_i) was calculated using the equation $K_i = 0.5 \times IC_{50}$ by assuming competitive inhibition in all cases, as substrate was investigated at a concentration equal to previously determined K_m value. The therapeutic total inhibitor concentration $[I]_{max}$, which is the C_{max}, in human plasma was obtained from pharmaceutical package inserts, the Handbook of

Anti-Tuberculosis Agents (http://dx.doi.org/10.1016/S1472-9792(08)70002-7), and a previously published report (Peloquin et al., 1996). $[I]_{max}$ / K_i values were calculated from K_i and reported $[I]_{max}$ values. Further, unbound plasma concentration ($[I]_{max,u}$) and total and unbound hepatic input concentrations ($[I]_{in}$ and $[I]_{in,u}$) were determined for CYP3A4 based on the reports (Ito et al., 2004 and Obach et al., 2006). The unbound fraction (f_u) of anti-TB drugs was obtained from a previously published report (Lakshminarayana et al., 2014).

5.3. Results and Discussion

According to the WHO guideline published in 2011 (http://whqlibdoc.who.int/publications/2011/9789241501583_eng.pdf), the anti-TB drugs are divided into five groups: first-line drugs, second-line parenteral drugs, fluoroquinolones, oral bacteriostatic second-line drugs, and other group 5 drugs. The choice of drug depends on the drug-susceptibility test or close contacts with MDR-TB, previous use of the drug in the patient, and the frequency of its use or documented background drug resistance in the setting. However, information on the CYP inhibitory potential for anti-TB drugs both *in vivo* and *in vitro* is limited. With this background, the potential for direct inhibition of twenty five anti-TB drugs on eight CYP specific reactions was investigated using human liver microsomes *in vitro*, and $[I]_{max}$ / K_i values were calculated to evaluate risks for clinical DDIs.

The percent of inhibition of anti-TB drugs at the highest concentration used on typical CYP reactions is shown in Fig. 5-1. The IC_{50} and $[I]_{max}$ / K_i values are shown in Tables 5-2 and 5-3, respectively. Of the drugs investigated in the present study, eight drugs inhibited one or more CYP reactions. The other seventeen drugs showed no IC_{50} values for all eight CYP reactions.

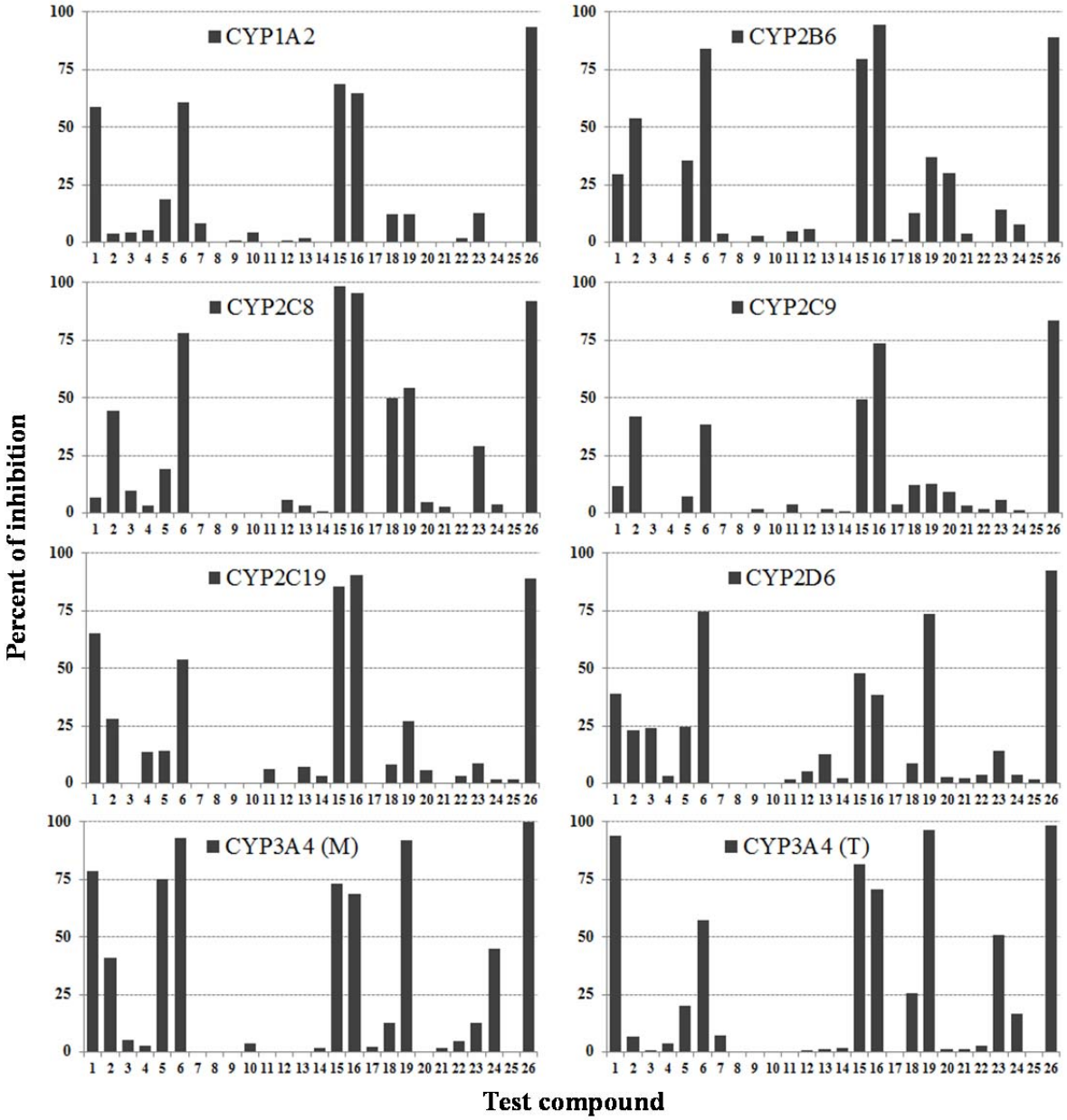

Fig. 5-1 Percent of inhibition of anti-tuberculosis drugs on typical CYP reactions.

Values are shown as the percent of inhibition at the highest concentration of the test compound. All inhibition data were calculated using the mean of data in duplicate. The test compound and concentration-range (μM) are as follows: (1) isoniazid (1–1000); (2) rifampicin (0.3–300); (3) ethambutol (0.3–300); (4) pyrazinamide (1–1000); (5) rifabutin (0.03–30); (6) rifapentine (0.3–300); (7) streptomycin (1–1000); (8) kanamycin (0.1–100); (9) amikacin (0.3–300); (10) capreomycin (1–1000); (11) levofloxacin (0.1–100); (12) moxifloxacin (0.1–100); (13) gatifloxacin (0.1–100); (14) ofloxacin (0.03–30); (15) ethionamide (1–1000); (16) prothionamide (0.3–300); (17) cycloserine (1–1000); (18) *p*-aminosalicylic acid (3–3000); (19) clofazimine (0.03–30); (20) linezolid (0.3–300); (21) amoxicillin (0.1–100); (22) clavulanate (0.3–300); (23) thioacetazone (0.1–100); (24) clarithromycin (0.03–30); (25) imipenem (0.1–100); (26) positive control.

Table 5-2 IC_{50} value of anti-tuberculosis drugs on typical CYP reactions.

Test compound	Concentration (μM)	IC_{50} (μM)							
		CYP1A2	CYP2B6	CYP2C8	CYP2C9	CYP2C19	CYP2D6	CYP3A4 (M)	CYP3A4 (T)
Isoniazid	1–1000	773	-	-	-	605	-	285	58.5
Rifampicin	0.3–300	-	237	-	-	-	-	-	-
Rifabutin	0.03–30	-	-	-	-	-	-	8.55	-
Rifapentine	0.3–300	246	64.2	115	-	214	81.6	23.0	232
Ethionamide	1–1000	524	396	110	-	195	-	451	282
Prothionamide	0.3–300	188	34.3	57.6	153	43.6	-	180	148
Clofazimine	0.03–30	-	-	14.1	-	-	4.54	0.275	0.304
Thioacetazone	0.1–100	-	-	-	-	-	-	-	98.0

-Not calculated

Table 5-3 Assessment of DDIs of anti-tuberculosis drugs on typical CYP reactions.

Test compound	Dose (mg)	$[I]_{max}$[a]		$[I]_{max} / K_i$[b]							
		(μg/mL)	(μM)	CYP1A2	CYP2B6	CYP2C8	CYP2C9	CYP2C19	CYP2D6	CYP3A4 (M)	CYP3A4 (T)
Isoniazid	300	8.00	58.4	0.15	-	-	-	0.19	-	0.41	2.0
Rifampicin	450	7.99	9.71	-	0.082	-	-	-	-	-	-
Rifabutin	600	0.724	0.855	-	-	-	-	-	-	0.20	-
Rifapentine	600	15.1	17.2	0.14	0.53	0.30	-	0.16	0.42	1.5	0.15
Ethionamide	500	12.5	75.2	0.29	0.38	1.4	-	0.77	-	0.33	0.53
Prothionamide	250	6.94	38.5	0.41	2.2	1.3	0.50	1.8	-	0.43	0.52
Clofazimine	200	0.408	0.862	-	-	0.12	-	-	0.38	6.3	5.7
Thioacetazone	150	1.59	6.73	-	-	-	-	-	-	-	0.14

[a]Total inhibitor concentration ($[I]_{max}$), which is the C_{max}, was obtained from pharmaceutical package inserts, the Handbook of Anti-Tuberculosis Agents, and a previously published report (Peloquin et al., 1996). [b]Inhibition constant (K_i) was calculated using the equation, $K_i = 0.5 \times IC_{50}$ by assuming competitive inhibition in all cases, as substrate was investigated at a concentration equal to previously determined Michaelis–Menten value. -Not calculated

The first-line drugs rifampicin and rifabutin inhibited CYP2B6 and CYP3A4 (M), respectively; however, the $[I]_{max}$ / K_i values were 0.20 or less. Isoniazid had inhibitory effects on four CYP reactions. The $[I]_{max}$ / K_i values for isoniazid on CYP1A2, CYP2C19, and CYP3A4 (M) were 0.41 or less. The highest $[I]_{max}$ / K_i value was 2.0 for CYP3A4 (T). Rifapentine widely inhibited CYP reactions. The $[I]_{max}$ / K_i values for rifapentine on CYP1A2, CYP2B6, CYP2C8, CYP2C19, CYP2D6, and CYP3A4 (T) were 0.53 or less, and the highest $[I]_{max}$ / K_i value was 1.5 for CYP3A4 (M). These results suggest that isoniazid and rifapentine may cause DDIs with CYP3A4. The difference in IC_{50} values between midazolam- and testosterone-mediated reactions is considered to reflect the difference in the CYP3A4-binding sites. Based on chemical inhibition characterizations and substrate correlation analyses, midazolam and testosterone seem to belong to two distinct groups of CYP3A4 substrates (Kenworthy et al., 1999).

The second-line injectable drugs kanamycin, amikacin, and capreomycin showed no inhibition on eight CYP reactions, and the fluoroquinolones levofloxacin, moxifloxacin, gatifloxacin, and ofloxacin also showed no inhibition on eight CYP reactions. These second-line injectable drugs and fluoroquinolones are often used to treat MDR-TB patients, and the results indicate that inhibition on CYP reactions by these drugs may not need to be taken into account in combination treatment for MDR-TB patients.

The orally administrated second-line drugs ethionamide and prothionamide widely inhibited the same CYP reactions. The $[I]_{max}$ / K_i values of ethionamide on CYP1A2, CYP2B6, CYP2C19, CYP3A4 (M), and CYP3A4 (T) were 0.77 or less, and those of prothionamide on CYP1A2, CYP2C9, CYP3A4 (M), and CYP3A4 (T) were 0.52 or less. The highest $[I]_{max}$ / K_i value for ethionamide was 1.4 on CYP2C8, and the highest $[I]_{max}$ / K_i values for prothionamide were 2.2, 1.8, and 1.3 on CYP2B6, CYP2C19, and CYP2C8, respectively. These inhibitory results suggest that prothionamide is likely to cause clinically

relevant DDIs with CYP2B6. The inhibition of CYP2C19 and CYP2C8 by prothionamide and that of CYP2C8 by ethionamide may cause DDIs. Ethionamide and prothionamide have a pyridine moiety in their chemical structure, as does isoniazid. Uncoupled pairs of nitrogen atoms in pyridine are considered to inhibit CYP (Lesca et al., 1978).

Of the group 5 drugs, thioacetazone inhibited CYP3A4 (T) reaction; however, the $[I]_{max}$ / K_i value was only 0.14. Clofazimine had inhibitory effects on four CYP reactions. The $[I]_{max}$ / K_i values for clofazimine were 0.38 on CYP2D6 and 0.12 on CYP2C8, and the highest $[I]_{max}$ / K_i values were 6.3 on CYP3A4 (M) and 5.7 on CYP3A4 (T). Authors (Horita and Doi, 2014) reported that the IC_{50} value of clofazimine on CYP3A4-mediated 7-benzyloxy-trifluoromethylcoumarin metabolism was nearly equal to the C_{max}, suggesting that clofazimine has an $[I]_{max}$ / K_i value of 1 or higher.

Further, total and unbound plasma concentrations ($[I]_{max}$ and $[I]_{max,u}$) and hepatic concentrations ($[I]_{in}$ and $[I]_{in,u}$) for CYP3A4 were calculated and [I] / K_i values were compared. These results are shown in Table 5-4. AUC ratios (1 + [I] / K_i values) for isoniazid calculated by $[I]_{max}$ and $[I]_{max,u}$ were from 1.41 to 3.0, and those by $[I]_{in}$ and $[I]_{in,u}$ were from 2.3 to 7.6. It is reported that isoniazid coadministration increased the total AUC of triazolam (substrate of CYP3A4) after a single oral dose by 1.5 folds (control (26.5 ng·h/mL) *vs* with isoniazid (38.6 ng·h/mL)) (Ochs et al., 1983). The use of total or unbound plasma concentration may be an adequate method because $[I]_{max}$ / K_i and $[I]_{max,u}$ / K_i values of isoniazid were identical with the AUC ratio. As clofazimine shows high [I] / K_i values by four methods, drugs metabolized by CYP3A4 should be carefully administered with clofazimine.

Table 5-4 Assessment of DDIs of anti-tuberculosis drugs on CYP3A4.

Test compound	f_u [a]	CYP3A4 (M)				CYP3A4 (T)			
		$[I]_{max} / K_i$	$[I]_{max,u} / K_i$ [b]	$[I]_{in} / K_i$ [c]	$[I]_{in,u} / K_i$ [d]	$[I]_{max} / K_i$	$[I]_{max,u} / K_i$ [b]	$[I]_{in} / K_i$ [c]	$[I]_{in,u} / K_i$ [d]
Isoniazid	0.99	0.41	0.41	1.4	1.3	2.0	2.0	6.6	6.6
Rifampicin	0.10	-	-	-	-	-	-	-	-
Rifabutin	0.15	0.20	0.030	10	1.6	-	-	-	-
Rifapentine	0.03	1.5	0.045	5.2	0.16	0.15	0.0044	0.51	0.015
Ethionamide	0.70	0.33	0.23	1.2	0.81	0.53	0.37	1.9	1.3
Prothionamide	0.40	0.43	0.17	1.4	0.55	0.52	0.21	1.7	0.67
Clofazimine	0.30	6.3	1.9	197	59	5.7	1.7	178	53
Thioacetazone	0.05	-	-	-	-	0.14	0.0069	0.94	0.047

[a]The unbound fraction (f_u) of anti-TB drugs was obtained from a previously published report (Lakshminarayana et al., 2014). [b]$[I]_{max,u}$ was calculated from $[I]_{max} \times f_u$. [c]$[I]_{in}$ was calculated from the equation, $[I]_{max} + k_a F_a D/Q_h$. The values of k_a (absorption rate constant), F_a (fraction absorbed from gut into portal vein), Q_h (hepatic blood flow rate), and R_B (blood-to-plasma concentration ratio) were assumed to be 0.1 min^{-1}, 1, 1610 ml min^{-1}, and 1, respectively, and D was dose. [d]$[I]_{in,u}$ was calculated from $[I]_{in} \times f_u$. -Not calculated

Of novel drugs and candidates currently undergoing clinical trials, bedaquiline (TMC-207), pretomanid (PA-824), and sutezolid have been reported to be substrates of CYP3A4 (Dooley et al., 2012). In addition, HIV protease inhibitors are substrates of CYP3A4 (Barry et a., 1999). Efavirenz, a non-nucleoside reverse transcriptase inhibitor, is a substrate of CYP3A4 and CYP2B6 (Barry et a., 1999; Ward et al., 2003). Considering the drug regimens for TB and co-infection with TB and HIV, the potential for CYP3A4 and CYP2B6 inhibition is particularly important. In conclusion, clofazimine and prothionamide are likely to cause clinically relevant DDIs when co-administered with products that are metabolized by CYP3A4 and CYP2B6, respectively. Isoniazid and rifapentine may cause DDIs via the inhibition of CYP3A4.

5.4. Chapter summary

The direct inhibitory potential of twenty five anti-tuberculosis drugs on eight CYP-specific reactions in human liver microsomes was investigated to predict *in vivo* DDIs from *in vitro* data. Rifampicin, rifabutin, and thioacetazone inhibited one CYP reaction. Isoniazid and clofazimine had inhibitory effects on four CYP reactions, and rifapentine, ethionamide, and prothionamide widely inhibited CYP reactions. Based on the inhibition constant (K_i) and the therapeutic total inhibitor concentrations $[I]_{max}$ of eight drugs in human plasma, $[I]_{max}$ / K_i values were calculated to evaluate clinical DDIs. The $[I]_{max}$ / K_i values were 0.20 or less for rifampicin, rifabutin, and thioacetazone; 0.15–2.0 for isoniazid; 0.14–1.5 for rifapentine; 0.29–1.4 for ethionamide; 0.41–2.2 for prothionamide; and 0.12–6.3 for clofazimine. The highest $[I]_{max}$ / K_i values were 2.0 for isoniazid on CYP3A4 [testosterone (T)]; 1.5 for rifapentine on CYP3A4 [midazolam (M)]; 1.4 for ethionamide on CYP2C8; 2.2, 1.8, and 1.3 for prothionamide on CYP2B6, CYP2C19, and CYP2C8, respectively; and 6.3 and 5.7 for clofazimine on CYP3A4 (M) and CYP3A4 (T), respectively. These drugs with high $[I]_{max}$ / K_i values lead to clinical DDIs. Considering the drug regimens for tuberculosis (TB) and co-infection with TB and human immunodeficiency virus, the inhibitory potential for CYP3A4 and CYP2B6 is particularly important. These results suggest that clofazimine and prothionamide are likely to cause clinically relevant DDIs when co-administered with products metabolized by CYP3A4 and CYP2B6, respectively. Isoniazid and rifapentine may cause DDIs with drugs metabolized by CYP3A4.

Chapter 6

Conclusion

First of all, we characterized the pharmacokinetics and metabolism of delamanid, a new anti-TB drug, in humans and animals. Eight metabolites (M1 to M8) produced by cleavage of its 6-nitro-2,3-dihydro-imidazo[2,1-*b*]oxazole moiety of delamanid were identified in the plasma after repeated oral administration. Delamanid was initially catalyzed to M1 and subsequently metabolized by three separate pathways. The primary biotransformation pathway of delamanid is to M1 and the major metabolite M1 is proposed to undergo subsequent metabolic reaction, including oxidations to M2 and M2 to M3 by CYP3A4 in humans. This route is very essential for the delamanid metabolism. Speculating the chemical structure of M1, it is proposed that delamanid is cleaved directly at the imidazooxazole moiety by some extrahepatic mechanism.

It is important to identify the enzymes responsible for the metabolism of delamanid in humans. The metabolism of delamanid was investigated *in vitro* using plasma and purified protein preparations from humans. A major metabolite, M1, was formed in the plasma by cleavage of the imidazooxazole moiety of delamanid. The rate of M1 formation increased with temperature (0−37°C) and pH (6.0−8.0). Delamanid was not converted to M1 in plasma filtrate, with a molecular mass cutoff of 30 kDa, suggesting that bioconversion is mediated by plasma proteins of higher molecular weight. When delamanid was incubated in plasma protein fractions separated by gel filtration chromatography, M1 was observed in the fraction consisting of albumin, γ-globulin, and α_1-acid glycoprotein. In pure preparations of these proteins, only HSA metabolized delamanid to M1. The formation of M1 followed Michaelis–Menten kinetics in both human plasma and HSA solution with similar K_m values: 67.8 μM in plasma and 51.5 μM in HSA. The maximum velocity and intrinsic clearance values for M1 were also comparable in plasma and HSA. These results strongly suggest that albumin is predominantly responsible for metabolizing delamanid to M1. The electron-poor carbon at

the C-5 position of the delamanid imidazooxazole structure is able to react with a nucleophile. Considering the fact that a delamanid analog without the nitro group was not metabolized by albumin, an electron-withdrawing nitro group of delamanid is suggested to be important for the propensity toward ring scission by albumin.

A novel drug for drug-resistant TB should be used for long-term administration as an add-on therapy to at least 3 or more other anti-TB drugs to prevent the development of resistance. It is therefore critical to understand the potential anti-TB drugs to inhibit or induced CYP enzymes. The ability of delamanid to inhibit or induce CYP enzymes was investigated *in vitro* using human liver microsomes or hepatocytes. The data suggest that delamanid is unlikely to cause clinically relevant DDIs when co-administered with products that are metabolized by the CYP enzyme system. Furthermore, the direct inhibitory potential of twenty five anti-tuberculosis drugs on eight CYP-specific reactions in human liver microsomes was investigated. The results suggest that clofazimine and prothionamide are likely to cause clinically relevant DDIs when co-administered with products metabolized by CYP3A4 and CYP2B6, respectively. Isoniazid and rifapentine may cause DDIs with drugs metabolized by CYP3A4.

To the best of our knowledge, this is the first report describing the *in vitro* mechanism of delamanid metabolism in human plasma. The new anti-TB drug delamanid is metabolized to M1 by albumin in plasma. We propose that delamanid degradation by albumin begins with a nucleophilic attack of amino acid residues on the electron-poor carbon at the 5 position of nitro-dihydro-imidazooxazole, followed by cleavage of the imidazooxazole moiety to form M1. This is a novel biotransformation.

Acknowledgements

本論文の作成にあたり、御懇篤なる御指導と御鞭撻を賜りました、徳島大学大学院医歯薬学研究部　薬科学部門　薬物治療学分野　教授　滝口祥令先生に謹んで感謝の意を表します。

本研究の遂行および本論文の作成に際し、終始過分の御便宜と有益な御助言を賜りました、大塚製薬株式会社　徳島研究所　代謝分析研究部　部長　梅原健博士、主任研究員　笹辺裕行博士、主任研究員　古川正幸博士、有機化学研究所　主任研究員　北野和良博士ならびに抗結核プロジェクトの皆様に厚く御礼申し上げます。

本研究の遂行に際し御協力を頂きました、大塚製薬株式会社　代謝分析研究部笹原克則氏、依田典朗氏、柴田昌和氏、小山紀之博士、平尾幸弘氏、近藤聡志氏、水野克彦氏、山村佳也氏をはじめ、代謝分析研究部の皆様に心より感謝いたします。

本研究遂行の機会ならびに多大の御便宜を賜りました、大塚製薬株式会社　徳島研究所　所長　樫山英二博士、小富正昭顧問ならびに山下修司博士に深く感謝の意を表します。

最後に、本論文の作成は、家族の支えなくしては成しえなかったものであります。ここに深く感謝いたします。

２０１５年６月

下川　義彦

References

Barry M, Mulcahy F, Merry C, Gibbons S, and Back D (1999) Pharmacokinetics and potential interactions amongst antiretroviral agents used to treat patients with HIV infection. *Clin Pharmacokinet* **36**:289–304.

Chang KC and Yew WW (2013) Management of difficult multidrug-resistant tuberculosis and extensively drug-resistant tuberculosis: update 2012. *Respirology* **18**:8–21.

Diacon AH, Dawson R, Hanekom M, Narunsky K, Venter A, Hittel N, Geiter LJ, Wells CD, Paccaly AJ, and Donald PR (2011) Early bactericidal activity of delamanid (OPC-67683) in smear-positive pulmonary tuberculosis patients. *Int J Tuberc Lung Dis* **15**:949–954.

Dogra M, Palmer BD, Bashiri G, Tingle MD, Shinde SS, Anderson RF, O'Toole R, Baker EN, Denny WA, and Helsby NA (2011) Comparative bioactivation of the novel anti-tuberculosis agent PA-824 in Mycobacteria and a subcellular fraction of human liver. *Br J Pharmacol* **162**:226–236.

Dooley KE, Kim PS, Williams SD, and Hafner R (2012) TB and HIV therapeutics: pharmacology research priorities. *AIDS Res Treat* 2012:874083.

Dooley KE, Luetkemeyer AF, Park JG, Allen R, Cramer Y, Murray S, Sutherland D, Aweeka F, Koletar SL, and Marzan F, et al.; AIDS Clinical Trials Group A5306 Study Team (2014) Phase I safety, pharmacokinetics, and pharmacogenetics study of the

antituberculosis drug PA-824 with concomitant lopinavir-ritonavir, efavirenz, or rifampin. *Antimicrob Agents Chemother* **58**:5245–5252.

Falzon D, Jaramillo E, Schünemann HJ, Arentz M, Bauer M, Bayona J, Blanc L, Caminero JA, Daley CL, Duncombe C, Fitzpatrick C, Gebhard A, Getahun H,Henkens M, Holtz TH, Keravec J, Keshavjee S, Khan AJ, Kulier R, Leimane V, Lienhardt C, Lu C, Mariandyshev A, Migliori GB, Mirzayev F, Mitnick CD, Nunn P,Nwagboniwe G, Oxlade O, Palmero D, Pavlinac P, Quelapio MI, Raviglione MC, Rich ML, Royce S, Rüsch-Gerdes S, Salakaia A, Sarin R, Sculier D, Varaine F,Vitoria M, Walson JL, Wares F, Weyer K, White RA, and Zignol M (2011) WHO guidelines for the programmatic management of drug-resistant tuberculosis: 2011 update. *Eur Respir J* **38**:516–528.

Gandhi NR, Andrews JR, Brust JCM, Montreuil R, Weissman D, Heo M, Moll AP, Friedland GH, and Shah NS (2012) Risk factors for mortality among MDR- and XDR-TB patients in a high HIV prevalence setting. *Int J Tuberc Lung Dis* **16**:90–97.

Ge GB, Ai CZ, Hu WB, Hou J, Zhu LL, He GY, Fang ZZ, Liang SC, Wang FY, and Yang L (2013) The role of serum albumin in the metabolism of Boc5: molecular identification, species differences and contribution to plasma metabolism. *Eur J Pharm Sci* **48**:360–369.

Gler MT, Skripconoka V, Sanchez-Garavito E, Xiao H, Cabrera-Rivero JL, Vargas-Vasquez DE, Gao M, Awad M, Park SK, Shim TS, Suh GY, Danilovits M, Ogata H, Kurve A, Chang J, Suzuki K, Tupasi T, Koh WJ, Seaworth B, Geiter LJ, and Wells CD (2012)

Delamanid for multidrug-resistant pulmonary tuberculosis. *N Engl J Med* **366**:2151–2160.

Horita Y and Doi N (2014) Comparative study of the effects of antituberculosis drugs and antiretroviral drugs on cytochrome P450 3A4 and P-glycoprotein. *Antimicrob Agents Chemother* **58**:3168–3176.

Ikeda T, Nishimura K, Taniguchi T, Yoshimura T, Hata T, Kashiyama E, Kudo S, Miyamoto G, Kobayashi H, Kobayashi S, Okazaki O, Hakusui H, Aoyama E, Yoshimura Y, Yamada Y, Yoshikawa M, Otsuka M, Niwa T, Kagayama A, Suzuki S, and Satoh T (2001) *In vitro* evaluation of drug interaction caused by enzyme inhibition. *Xenobio Metabol and Dispos* **16**:115–126.

Imaoka S, Yamada T, Hiroi T, Hayashi K, Sakaki T, Yabusaki Y, and Funae Y (1996) Multiple forms of human P450 expressed in Saccharomyces cerevisiae. Systematic characterization and comparison with those of the rat. *Biochem Pharmacol* **51**:1041–1050.

Ito K, Brown HS, and Houston JB (2004) Database analyses for the prediction of *in vivo* drug-drug interactions from *in vitro* data. *Br J Clin Pharmacol* **57**:473–486.

Kenworthy KE, Bloomer JC, Clarke SE, and Houston JB (1999) CYP3A4 drug interactions: correlation of 10 in vitro probe substrates. *Br J Clin Pharmacol* **48:** 716–727.

Kurono Y, Maki T, Yotsuyanagi T, and Ikeda K (1979) Esterase-like activity of human

serum albumin: structure-activity relationships for the reactions with phenyl acetates and pnitrophenyl esters. *Chem Pharm Bull (Tokyo)* **27**:2781–2786.

Lakshminarayana SB, Huat TB, Ho PC, Manjunatha UH, Dartois V, Dick T, and Rao SP (2014) Comprehensive physicochemical, pharmacokinetic and activity profiling of anti-TB agents. *J Antimicrob Chemother* **70**:857–867.

LeCluyse EL, Audus KL, and Hochman JH (1994) Formation of extensive canalicular networks by rat hepatocytes cultured in collagensandwich configuration. *Am J Physiol* **266**:C1764–C1774.

LeCluyse EL, Bullock PL, Parkinson A, and Hochman JH (1996) Cultured rat hepatocytes. *Pharm Biotechnol* **8**:121–159.

Lesca P, Lecointe P, Paoletti C, and Mansuy D (1978) Ellipticines as potent inhibitors of aryl hydrocarbon hydroxylase: their binding to microsomal cytochromes P450 and protective effect against benzo(a)pyrene mutagenicity. *Biochem Pharmacol* **27**:1203–1209.

Liyasova MS, Schopfer LM, and Lockridge O (2010) Reaction of human albumin with aspirin *in vitro*: mass spectrometric identification of acetylated lysines 199, 402, 519, and 545. *Biochem Pharmacol* **79**:784–791.

Lockridge O, Xue W, Gaydess A, Grigoryan H, Ding S-J, Schopfer LM, Hinrichs SH, and Masson P (2008) Pseudo-esterase activity of human albumin: slow turnover on

tyrosine 411 and stable acetylation of 82 residues including 59 lysines. *J Biol Chem* **283**:22582–22590.

Ma S-F, Anraku M, Iwao Y, Yamasaki K, Kragh-Hansen U, Yamaotsu N, Hirono S, Ikeda T, and Otagiri M (2005) Hydrolysis of angiotensin II receptor blocker prodrug olmesartan medoxomil by human serum albumin and identification of its catalytic active sites. *Drug Metab Dispos* **33**:1911–1919.

Madan A, Dehaan R, Mudra D, Carroll K, LeCluyse E, and Parkinson A (1999) Effect of cryopreservation on cytochrome P-450 enzyme induction in cultured rat hepatocytes. *Drug Metab Dispos* **27**:327–335.

Madan A, Graham RA, Carroll KM, Mudra DR, Burton LA, Krueger LA, Downey AD, Czerwinski M, Forster J, Ribadeneira MD, Gan LS, LeCluyse EL, Zech K, Robertson P Jr, Koch P, Antonian L, Wagner G, Yu L, and Parkinson A (2003) Effects of prototypical microsomal enzyme inducers on cytochrome P450 expression in cultured human hepatocytes. *Drug Metab Dispos* **31**:421–431.

Matsumoto M, Hashizume H, Tomishige T, Kawasaki M, Tsubouchi H, Sasaki H, Shimokawa Y, and Komatsu M (2006) OPC-67683, a nitro-dihydro-imidazooxazole derivative with promising action against tuberculosis *in vitro* and in mice. *PLoS Med* **3**:e466.

Means GE and Bender ML (1975) Acetylation of human serum albumin by p-nitrophenyl acetate. *Biochemistry* **14**:4989–4994.

Miyamoto G, Shimokawa Y, Itose M, Koga T, Hirao Y, and Kashiyama E (2005) Unique PK profile of OPC-67683, a new potent anti-tuberculous drug, in 45th Interscience Conference on Antimicrobial Agents and Chemotherapy; 2005 December 16–19; Washington, DC. Poster F-1466, American Society for Microbiology, Washington, DC.

Mudra DR and Parkinson A (2001) Preparation of hepatocytes. *Curr Protoc Toxicol* Chapter 14, Unit 14.2.

Obach RS, Walsky RL, Venkatakrishnan K, Gaman EA, Houston JB, and Tremaine LM (2006) The utility of *in vitro* cytochrome P450 inhibition data in the prediction of drug-drug interactions. *J Pharmacol Exp Ther* **316**:336–348.

Obach RS, Walsky RL, and Venkatakrishnan K (2007) Mechanism-based inactivation of human cytochrome P450 enzymes and the prediction of drug–drug interactions. *Drug Metab. Dispos* **35**:246–255.

Ochs HR, Greenblatt DJ, and Knüchel M (1983) Differential effect of isoniazid on triazolam oxidation and oxazepam conjugation. *Br J Clin Pharmacol* **16**:743-746.

Ohta N, Kurono Y, and Ikeda K (1983) Esterase-like activity of human serum albumin II: reaction with N-trans-cinnamoylimidazoles. *J Pharm Sci* **72**:385–388.

Ozeki Y, Kurono Y, Yotsuyanagi T, and Ikeda K (1980) Effects of drug binding on the

esterase activity of human serum albumin: inhibition modes and binding sites of anionic drugs. *Chem Pharm Bull (Tokyo)* **28**:535–540.

Paccaly A, Petersen C, Patil S, Bricmont P, Kim J, Harlin M, and Wells C (2012) Absence of clinically relevant drug interaction between delamanid, a new drug for multidrug-resistant tuberculosis (MDR-TB) and tenofovir or lopinavir/ritonavir in healthy subjects, in 19th International AIDS Conference; 2012 July 22–27; Washington, DC. Poster WEPE043, International AIDS Society, Geneva, Switzerland.

Peloquin CA, Nitta AT, Berning SE, Iseman MD, and James GT (1996) Pharmacokinetic evaluation of thiacetazone. *Pharmacotherapy* **16**:735–741.

Petersen C, Paccaly A, Kim J, Roth S, Stoltz R, and Wells C (2012) Delamanid, a new drug for multi-drug resistant tuberculosis (MDR-TB), and efavirenz do not show clinically relevant drug interactions in healthy subjects, in 52nd Interscience Conference on Antimicrobial Agents and Chemotherapy; 2012 September 9–12; San Francisco, CA. Abstract A-1255, American Society for Microbiology, Washington, DC.

Quistorff B, Dich J, and Grunnet N (1990) Preparation of isolated rat liver hepatocytes. *Methods Mol Biol* **5**:151–160.

Rainsford KD, Ford NL, Brooks PM, and Watson HM (1980) Plasma aspirin esterases in normal individuals, patients with alcoholic liver disease and rheumatoid arthritis: characterization and the importance of the enzymic components. *Eur J Clin Invest*

10:413–420.

Robertson P, Decory HH, Madan A, and Parkinson A (2000) *In vitro* inhibition and induction of human hepatic cytochrome P450 enzymes by modafinil. *Drug Metab Dispos* **28**:664–67.

Sakurai Y, Ma S-F, Watanabe H, Yamaotsu N, Hirono S, Kurono Y, Kragh-Hansen U, and Otagiri M (2004) Esterase-like activity of serum albumin: characterization of its structural chemistry using p-nitrophenyl esters as substrates. *Pharm Res* **21**:285–292.

Salvi A, Carrupt P-A, Mayer JM, and Testa B (1997) Esterase-like activity of human serum albumin toward prodrug esters of nicotinic acid. *Drug Metab Dispos* **25**:395–398.

Sasaki H, Haraguchi Y, Itotani M, Kuroda H, Hashizume H, Tomishige T, Kawasaki M, Matsumoto M, Komatsu M, and Tsubouchi H (2006) Synthesis and antituberculosis activity of a novel series of optically active 6-nitro-2,3-dihydroimidazo-[2,1-b]oxazoles. *J Med Chem* **49**:7854–7860.

Schweikl H, Taylor JA, Kitareewan S, Linko P, Nagorney D, and Goldstein JA (1993) Expression of CYP1A1 and CYP1A2 genes in human liver. *Pharmacogenetics* **3**:239–249.

Skripconoka V, Danilovits M, Pehme L, Tomson T, Skenders G, Kummik T, Cirule A, Leimane V, Kurve A, Levina K, Geiter LJ, Manissero D, and Wells CD (2013) Delamanid improves outcomes and reduces mortality in multidrug-resistant

tuberculosis. *Eur Respir J* **41**:1393–1400.

Sogorb MA, Carrera V, and Vilanova E (2004) Hydrolysis of carbaryl by human serum albumin. *Arch Toxicol* **78**:629–634.

Sudlow G, Birkett DJ, and Wade DN (1976) Further characterization of specific drug binding sites on human serum albumin. *Mol Pharmacol* **12**:1052–1061.

Sultatos LG, Basker KM, Shao M, and Murphy SD (1984) The interaction of the phosphorothioate insecticides chlorpyrifos and parathion and their oxygen analogues with bovine serum albumin. *Mol Pharmacol* **26**:99–104.

Theodore PJ (1996) *All about Albumin. Biochemistry, Genetics, and Medical Applications*, Academic Press, New York.

Wang RW, Newton DJ, Liu N, Atkins WM, and Lu AYH (2000) Human cytochrome P450 3A4: *in vitro* drug–drug interaction patterns are substrate-dependent. *Drug Metab Dispos* **28**:360–366.

Ward BA, Gorski JC, Jones DR, Hall SD, Flockhart DA, and Desta Z (2003) The cytochrome P450 2B6 (CYP2B6) is the main catalyst of efavirenz primary and secondary metabolism: implication for HIV/AIDS therapy and utility of efavirenz as a substrate marker of CYP2B6 catalytic activity. *J Pharmacol Exp Ther* **306**:287–300.

Watanabe H, Tanase S, Nakajou K, Maruyama T, Kragh-Hansen U, and Otagiri M (2000)

Role of arg-410 and tyr-411 in human serum albumin for ligand binding and esterase-like activity. *Biochem J* **349**:813–819.

Wolfbeis OS and Gurakar A (1987) The effect of fatty acid chain length on the rate of arylester hydrolysis by various albumins. *Clin Chim Acta* **164**:329–337.